R. & M. No. 2591
(10,895)
A.R.C. Technical Report

MINISTRY OF SUPPLY

AERONAUTICAL RESEARCH COUNCIL
REPORTS AND MEMORANDA

The Solution of Lifting-Plane Problems by Vortex-Lattice Theory

By

V. M. FALKNER, B.Sc., A.M.I.Mech.E.,
of the Aerodynamics Division, N.P.L.

WITH SEVEN APPENDICES

LONDON: HER MAJESTY'S STATIONERY OFFICE
1953
PRICE 10s. 6*d*. NET

The Solution of Lifting-Plane Problems by Vortex-Lattice Theory

By

V. M. FALKNER, B.Sc., A.M.I.Mech.E.
of the Aerodynamics Division, N.P.L.

WITH SEVEN APPENDICES

Reports and Memoranda No. 2591

September, 1947

Summary.—The report describes in detail the methods by which the principles of vortex-lattice theory, introduced in a previous report, R. & M. 1910[1], are applied to the calculation of the aerodynamic loading of wings by lifting-plane theory. The scope of the paper is limited to the application of these principles to symmetrical incidence solutions and symmetrical and anti-symmetrical wing twist solutions, for which standard solutions can be treated by comparatively simple loading functions, The effect of discontinuity of direction of leading or trailing edge cannot be avoided even in the simplest solutions, and it has been found necessary to include an investigation of this problem in order to cover the prescribed usage of the method. Special standard functions tabulated in another report are used to allow for the rounding off effects due to change of direction of leading or trailing edge. The general problem of discontinuities is under investigation and will be dealt with in a later report.

A comprehensive set of solutions for a delta wing is included in the report in order to show the convergence of and relation between solutions of varying complexity, and to indicate which solution should be used in order to satisfy the accuracy prescribed for any given problem. The case of the delta wing is not completely general, and the exposition in respect to induced drag and yawing moment will be completed in a later report.

1. *Introduction.*—In R. & M. 1910[1] an account has been given of the principles by which lifting-plane solutions for the aerodynamic loading of wings can be calculated by concentrating the equivalent vortex sheet, including the wake, into a number of elements of line vorticity arranged in a lattice and using numerical integration to compute the total downwash at selected points on the wing surface. The present report, which is based mainly on experience gained since publication of the previous report, has been written for the purpose of describing in detail the methods used in carrying out the calculations.

After standard and modified formulae, the scope of the work, and possible variations of the lattice have been specified, the paper continues by describing in detail how the control points —at which the tangential flow condition is expressed—are chosen on the wing surface; how the equations in the unknown variables of the loading formula are formed and solved; and how the properties of the wing are calculated from the known values of the coefficients in the loading formula.

Solutions of varying complexity are obtained by alteration of the chordwise or spanwise spacing of the lattice, and, in order to give guidance as to the most suitable procedure for a given problem, a large number of solutions has been worked out for a wing in the shape of an equilateral triangle, the choice being made as representative of a sweptback wing of small aspect ratio. It is now known that there are disadvantages in the use of pointed tips for theoretical investigations, one of the main objections being that it is exceedingly difficult to define what the accurate potential solution should be, and the form of the loading functions, in the region of the tips. In the chordwise direction, for instance, it would be necessary for a mathematical solution to define to close accuracy the position on the chord of the local aerodynamic centre

in the region near the tips, whereas, then the chord tends to zero, even a large variation of local aerodynamic centre in terms of the chord would have no appreciable effect on the general properties of the wing.

The writer has drawn attention to this matter in another report[2], and, from an examination of solutions based on alternative functions, has concluded that the solutions given here, which are based on formulae not strictly applicable to wings with pointed tips, are accurate as far as overall effects are concerned, any error being confined mainly to uncertainties in the local aerodynamic centre and lift coefficient in the region of the tips. Apart from this limitation, the solutions serve the main purpose of giving a comparable set of solutions representative of normal application of the method to sweptback wings without pointed tips.

1.1. The report is limited to a discussion of symmetrical and anti-symmetrical solutions for flat and twisted wings in straight flight without camber and without discontinuities other than those of direction of leading or trailing edges. The general principles of vortex lattice theory as described in the report are, however, of universal application, and later developments will be concerned mainly with variations of loading functions and downwash tables, and with methods for specifying artificial gradients for use in the tangential flow condition, in order to represent easily the effect of camber, flaps, or other devices.

It must again be emphasised that the work is primarily concerned with potential flow, the basic aerofoil profile being a straight line with a two-dimensional value of $dC_L/d\alpha = 2\pi$. The question of correction factors to allow for the effects of viscosity is not dealt with in this report. In order to make the basis of the work quite clear, particular attention is directed to the fact that the lattice is used only as part of the process for finding the values of the unknown coefficients in the formula for the vortex sheet, and that the properties of the wing are all derived subsequently from the lifting plane solution represented by the vortex sheet.

2. *Formula and Scope of Work.*—The formula used previously for the vortex sheet representing the wing surface and the wake is

$$\begin{aligned}\frac{kc}{8sV\tan\alpha} &= \sqrt{1-\eta^2}\cot\tfrac{1}{2}\Theta\,[a_0 + b_0\eta + c_0\eta^2 + d_0\eta^3 + \ldots.] \\ &+ \sqrt{1-\eta^2}\sin\Theta\,[a_1 + b_1\eta + c_1\eta^2 + d_1\eta^3 + \ldots.] \\ &+ \sqrt{1-\eta^2}\sin 2\Theta\,[a_2 + b_2\eta + c_2\eta^2 + d_2\eta^3 + \ldots.]. \quad .. \quad .. \quad (1)\end{aligned}$$

It will be appreciated that the success of the method depends upon obtaining a rapidly convergent solution, and it is necessary to examine the limitations of the formula from this point of view. It will be obvious that problems involving discontinuities of downwash, which may be due either to abrupt changes in chord or spanwise incidence, or to deflected control surfaces, will not fall within the scope of the formula. These discontinuities would normally be absent in the primary consideration of the effects of incidence. There is, however, another important discontinuity which cannot be avoided, that is, the sudden change of direction of the leading or trailing edge which occurs with tapered wings, usually near the wing centre, and occasionally along the span, and which is most marked in its effects for any wing when sweepback or sweepforward is present.

An independent unpublished investigation of the potential solution for the loading of two infinite Vee wings has shown that, at a discontinuity of direction of leading or trailing edge, the formula for the vortex strength should be suitable for expressing discontinuities or irregularities in the following quantities or their rate of change:—(a) circulation, (b) induced downwash, (c) local lift coefficient and (d) position of the local aerodynamic centre in terms of the chord. The exact nature of each of these irregularities is difficult to define mathematically, but it is believed that satisfactory results will be obtained by making some or all as nearly as possible simple discontinuities in the rate of change of the function in the spanwise direction.

2.1. The formula (1) is not suitable for the general representation of the four discontinuities, and special additional loading functions, termed P functions, have been calculated and tabulated in Ref. 7. These special functions are associated with distributions of induced downwash calculated by lifting-line theory, which have a discontinuity of rate of change in the spanwise direction, the choice being mainly influenced by the necessity for the satisfactory calculation of induced drag and yawing moment. The P functions, which appear to fulfil their purpose admirably, can be combined to represent a polygonal distribution of induced downwash with corners spaced as small as 0·05 semispan, although when used with the 0·1 semispan spaced lattice, the spacing of the corners requires widening to 0·1 semispan.

The revised formula for the vortex sheet which represents the wing surface and the wake without discontinuities other than those of direction of the leading or trailing edge, is, therefore, written as follows, the following modifications also being included:—(a) tan α is replaced by the more accurate function sin α and (b) revised definitions for F_0, F_1, and F_2 are used:—

$$\frac{kc}{8sV \sin \alpha} = F_0 \cot \tfrac{1}{2}\Theta + F_1 \sin \Theta + F_2 \sin 2\Theta \quad .. \quad .. \quad .. \quad .. \quad .. \quad (2)$$

where
$$F_0 = \sqrt{(1 - \eta^2)}\,[a_0 + b_0\eta + c_0\eta^2 + d_0\eta^3 + \ldots.] + p_0P$$
$$F_1 = \sqrt{(1 - \eta^2)}\,[a_1 + b_1\eta + c_1\eta^2 + d_1\eta^3 + \ldots.] + p_1P$$
$$F_2 = \sqrt{(1 - \eta^2)}\,[a_2 + b_2\eta + c_2\eta^2 + d_2\eta^3 + \ldots.] + p_2P$$

and P is a combination of special functions to suit each individual problem, the origin of which will be described below when specific problems are under consideration. A similar form, but with sin α removed, applies for the zero lift solution.

The term ' standard solution ' will be applied to any solution derived from equation (2) which excludes the P functions. Values of the standard loading functions up to $\eta^{10}\sqrt{(1 - \eta^2)}$ are given for $\eta = 0\ (0{\cdot}025)\ 1$ in Table 1.

3. *Standard Derived Formulae.*—The method of derivation of the formulae for the circulation and the lift coefficient is described in Appendix II. The analysis leads to the following, which are correct for an unlimited number of terms chordwise:—

$$K/4sV = \pi\,[F_0 + \tfrac{1}{2}F_1] \quad .. \quad .. \quad .. \quad .. \quad .. \quad .. \quad .. \quad .. \quad (3)$$

$$dC_L/d\alpha = \frac{1}{2}\frac{\pi^2 s^2}{S}\,[8a_0 + 4a_1 + 2c_0 + c_1 + e_0 + 0{\cdot}5e_1 + 0{\cdot}625g_0$$
$$+ 0{\cdot}3125g_1 + 0{\cdot}4375i_0 + 0{\cdot}21875i_1$$
$$+ 0{\cdot}328125k_0 + 0{\cdot}1640625k_1]. \quad .. \quad .. \quad .. \quad .. \quad .. \quad .. \quad (4)$$

Anti-symmetrical terms add nothing to the lift coefficient.

The formulae for rolling moment with unlimited terms chordwise and five anti-symmetrical terms spanwise, is obtained in a similar way:—

$$C_l = -\frac{1}{2}\frac{\pi^2 s^2}{S}\,[b_0 + 0{\cdot}5b_1 + 0{\cdot}5d_0 + 0{\cdot}25d_1 + 0{\cdot}3125f_0$$
$$+ 0{\cdot}15625f_1 + 0{\cdot}21875h_0 + 0{\cdot}109375h_1$$
$$+ 0{\cdot}1640625j_0 + 0{\cdot}08203125j_1]. \quad .. \quad .. \quad .. \quad .. \quad .. \quad .. \quad (5)$$

The position of the centre of pressure of the half wing symmetrical loading, in terms of the semispan, unlimited terms chordwise and six terms spanwise, is

$$\frac{32}{\pi}\frac{N}{D}, \qquad \ldots \quad (6)$$

where $N = 0{\cdot}3\dot{3}\ (a_0 + \frac{1}{2}a_1) + 0{\cdot}13\dot{3}\ (c_0 + \frac{1}{2}c_1) + 0{\cdot}076190\ (e_0 + \frac{1}{2}e_1)$
$+ 0{\cdot}050794\ (g_0 + \frac{1}{2}g_1) + 0{\cdot}036941\ (i_0 + \frac{1}{2}i_1)$
$+ 0{\cdot}028416\ (k_0 + \frac{1}{2}k_1) \qquad \ldots \quad (7)$

and $D = 8\ (a_0 + \frac{1}{2}a_1) + 2\ (c_0 + \frac{1}{2}c_1) + (e_0 + \frac{1}{2}e_1)$
$+ 0{\cdot}625\ (g_0 + \frac{1}{2}g_1) + 0{\cdot}4375\ (i_0 + \frac{1}{2}i_1)$
$+ 0{\cdot}328125\ (k_0 + \frac{1}{2}k_1). \qquad \ldots \quad (8)$

Local aerodynamic centre, unlimited terms chordwise and spanwise:—

$$0{\cdot}25\ \frac{F_0 + F_1 - \frac{1}{2}F_2}{F_0 + \frac{1}{2}F_1}\ \text{chord.} \qquad \ldots \quad (9)$$

The induced drag is calculated by using a simplification which follows from Munk's Stagger Theorem, and which can be readily demonstrated from the properties of the rectangular vortex. The induced drag due to the vortex lattice on any wing is the same as if the bound vortices were moved backwards or forwards until concentrated in a single line transverse to the wind direction, and the lifting line formula can be applied directly if the circulation is expressed by the terms of a Fourier series. The relation between the coefficients of the lifting plane formula and the lifting line notation is given in Appendix 1. To obtain the induced drag, the values of $A_1, A_2, \ldots A_n$, are first calculated, and it then follows that

$$C_{Di} = \pi A\ \Sigma n A_n^2 \text{ or } \frac{1}{\pi A}\ C_L^2\left[\frac{\Sigma n A_n^2}{A_1^2}\right]. \qquad \ldots \quad (10)$$

The local lift coefficient per radian incidence is

$$C_{LL} = 4\pi\ [F_0 + \tfrac{1}{2}F_1]/(c/2s) \qquad \ldots \quad (11)$$

and per unit C_L

$$C_{LL} = 4\pi\ [F_0 + \tfrac{1}{2}F_1]/(c/2s)\ (dC_L/d\alpha). \qquad \ldots \quad (12)$$

The formulae for special values of the local lift coefficient at the median section and at the tip are given in Appendix III.

The exact method of calculation of the yawing moment for a wing with combined symmetrical and anti-symmetrical loading has not yet been worked out, but a first approximation is obtained by calculating $A_1, A_2, \ldots A_n$, and using the following formula, the derivation of which from lifting line theory is given in Appendix IV:—

$$C_n = \frac{\pi s^2}{S}\ [3A_1A_2 + 5A_2A_3 + \ldots\ldots (2n+1)\ A_nA_{n+1} + \ldots.]. \qquad \ldots \quad (13)$$

The pitching moment is derived from the aerodynamic centre, which, together with other properties of the wing, is usually obtained by numerical integration, examples of which are given below.

The complete integrals on which some of the formulae of this paragraph are based, are given in Table 5.

3.1. The formulae of section 3 apply to the standard solutions in which the P functions are omitted. We now consider what modifications are necessary when the latter are included. So wide a range is covered by the P functions that it will only be possible here to define the methods by which the necessary modifications are made, but these will be followed by examples which will make the process clear.

The expressions for $K/4sV$ and the local aerodynamic centre automatically include the effects of the P functions. The value of $dC_L/d\alpha$ is increased by $\frac{1}{2}\frac{\pi^2 s^2}{S} T_{16} (p_0 + \frac{1}{2}p_1)$ for the symmetrical solution, the value of C_l by $-\frac{1}{2}\frac{\pi^2 s^2}{S} T_{18} (p_0 + \frac{1}{2}p_1)$ for the anti-symmetrical solution, and the position of the centre of pressure of the half wing symmetrical loading is modified by adding $T_{19} (p_0 + \frac{1}{2}p_1)$ to N and $T_{16} (p_0 + \frac{1}{2}p_1)$ to D, where T_{16}, T_{18}, and T_{19} are given in Table 8 of Ref. 7 for the original P functions and can be calculated as in Table 46 for any combination of P functions. The expressions for induced drag and yawing moment are only valid if the addition of the P functions leaves the circulation unchanged, *i.e.*, if $p_0 + \frac{1}{2}p_1 = 0$. The general case will later be given special treatment.

4. *Range of Solutions.*—The solutions described here have been based on three layouts, defined as the 21-vortex, 126-vortex, and 328-vortex respectively. An 84 layout, used frequently in early work, may still be of value for straight wings, but for sweptback wings has been discarded in favour of the 126, which has proved to be more accurate. The numeral indicates the total number of vortices which represent the wing, and the patterns for the four solutions, some of which have appeared in previous reports, are now collected together in concise form in Figs. 1 and 2.

The 21-vortex solution, known alternatively from the location of load line and control points as a $\frac{1}{4}/\frac{3}{4}$ solution, is the simplest which it is thought advisable to use. This solution, although defective in some respects, can be regarded as a true first approximation to lifting plane theory, to which the more elaborate solutions are closer approximations. Although it is possible to use a pattern lying between the 21 and 84 or 126, it will be seen from the work below that the advantages of the latter are so marked that any intermediate solution would not be worth consideration.

5. *Position of Control Points.*—The position of the control points on the wing depends upon the layout to be used, as well as the circumstances of the problem. For the 21-vortex layout, equivalent to the use of one term, $\cot \frac{1}{2}\theta$, in the chordwise direction, or $F_1 = F_2 = 0$, the control points must be on the $\frac{3}{4}$-chord line in order that this solution shall fall into proper relationship with the sequence of operations used to separate the chordwise continuous vorticity into its separate line vortices.

A general description of the method, which is based on two-dimensional considerations, is given in section 7 of R. & M. 1910. It can easily be shown that, with the continuous two-dimensional chordwise loading defined by $\cot \frac{1}{2}\theta$ concentrated to a line vortex at the $\frac{1}{4}$-chord, the $\frac{3}{4}$-chord is the only position where the downwashes are the same for the continuous and concentrated loadings.

For the 84 or other vortex patterns, each control point must be placed at the midpoint of one of the rectangles of the lattice, giving three possible chordwise positions for the 84, five for the 126, and 7 for the 328. Usually, the use of two or three chordwise terms in formula (1) requires the same number of chordwise positions for the control points, and the recommended positions are given in Table 4. It should be stated that errors in the computed downwash appear first for those pivotal points which are located over the forward part of the wing, where the intensity of loading is greater. For this reason, superior accuracy results from directing the control points towards the rear of the wing, as with the 126-vortex lattice.

5.1. The optimum location of control points in the spanwise direction has been determined by experience. For any layout spaced at 0·1 semispan, no point at 0·5 chord or behind should be nearer the tip than $0{\cdot}8\eta$, and no point forward of 0·5 chord should be nearer than $0{\cdot}7\eta$. If the spacing be halved to 0·05 semispan, the points may move to 0·9 and 0·8 respectively. These limitations are due to the fact that, if points were placed nearer the tip, they would be too near the edge of the lattice for a reliable calculation of downwash to result.

With the 21-vortex lattice it has been found hitherto that the points can be placed at any intersection of the $\frac{3}{4}$-chord with the centre line of a vortex. With the 84, 126, and 328 patterns, there is an additional limitation which depends upon the loading functions used. For either symmetrical or anti-symmetrical solutions which use the standard sequence $\sqrt{(1-\eta^2)}$, $\eta\sqrt{(1-\eta^2)}$, $\eta^2\sqrt{(1-\eta^2)}$, . . . , no control point should be placed nearer than 2 vortex widths spanwise to the point where there is a sudden change of direction of leading or trailing edge, such as occurs at the median section of the wings of Figs. 1, 4. If the P functions are added, or other special functions which serve the same purpose, the rounding-off effect at the discontinuity is allowed for, and it is then desirable to place a control point as near the discontinuity as possible.

5.2. Following these principles, the recommendations for a symmetrical solution for a wing with main change of direction at or near the centre are as follows:—With standard loading functions $\sqrt{(1-\eta^2)}$, $\eta^2\sqrt{(1-\eta^2)}$, $\eta^4\sqrt{(1-\eta^2)}$, use $\eta = 0{\cdot}2, 0{\cdot}5, 0{\cdot}8$ or $\eta = 0{\cdot}2, 0{\cdot}6, 0{\cdot}8$. If more functions of the same kind are used, or if additional relations are required, a suggested sequence is 0·2, 0·5, 0·7, 0·8; 0·2, 0·4, 0·5, 0·7, 0·8; or 0·2, 0·6, 0·7, 0·8; 0·2, 0·4, 0·6, 0·7, 0·8. When the P functions are added it is necessary to include points at $\eta = 0$ and perhaps 0·1. Similar principles apply when the discontinuity is away from the centre, in all cases the standard solution avoiding control points in the immediate vicinity of the discontinuity.

The procedure for the anti-symmetrical case is generally the same, but there may be a simplification when the discontinuity is at the wing centre, for in this case the downwash is zero at $\eta = 0$ and the standard functions may give a satisfactory solution.

A more general treatment of the problem will be made in a later report.

5.3. It should be stated that there are two main reasons why the spacing of the lattice, defined in terms of chord and span, should be constant over the wing:—(a) the overall accuracy depends to a certain extent on the averaging effect due to the use of a number of line vortices arranged in a uniform pattern and (b) no control point could be located in the region of a change of lattice spacing.

It is essential that the same number of chordwise points are used at each spanwise station as, otherwise, experience shows that a false solution might result. The exclusion of the term $\eta^4\sqrt{(1-\eta^2)}$ is not recommended on account of the possibility of error.

6. *Formation of Equations.*—At each control point, the total downwash is calculated by means of the lattice in terms of the unknown coefficients in relation (2), and is equated to the local slope of the plate representing the aerofoil profile. A set of simultaneous equations is thus obtained in the unknown variables.

The equations are formed in the following way. It is first necessary to construct a table of distances on which the calculations are to be based. For example, Table 6 gives these distances for the tapered and sweptback wing of Fig. 1; they are (a) the distance back, parallel to the wind direction, of datum to leading edge, and (b) the chord, both expressed in terms of the span, for $\eta = 0\ (0{\cdot}05)\ 1$.

The datum is any convenient line transverse to the wind direction, in this case passing through the apex of the wing. As the spacing is 0·1s, the value $\eta = 0{\cdot}9625$, at which the corrector vortex is located, must also be included. If the lattice spacing had been $\eta = 0{\cdot}05$, the table would be the same except that $\eta = 0{\cdot}98125$, the revised position for the corrector vortex, would be included.

6.1. The procedure for the 21-lattice is given in Table 2. Consider the total downwash at the control point 1 of Fig. 1, located at $\eta = 0{\cdot}2$, due to the spanwise loading function $a_0\sqrt{(1-\eta^2)}\cot\frac{1}{2}\Theta$. Row 2 gives positions on the span; row 3 the distances back, in terms of the semi-width of vortex, of the individual vortices, obtained from Table 6 by the formula $40a + 10b$; row 4 the relative displacements of the vortices from point 1, located at $\frac{3}{4}$-chord, or $[0{\cdot}2, 9{\cdot}550]$, obtained by subtracting $9{\cdot}550$ from row 3; row 6 gives the downwash factors due to the displacements of row 5, obtained by taking readings from tables of downwash for a rectangular vortex (*see* Appendix VI) for the figures of row 4, the entry opposite $0{\cdot}2$ starboard being used with table $y = 0$, those opposite $0{\cdot}1$ and $0{\cdot}3$ starboard with $y = 2$, and so on up to $0{\cdot}9$ port and starboard. The entries for $\eta = 0{\cdot}9625$ require special treatment as they refer to vortices which are only one-quarter of the standard width. In consequence, the figure of row 4, and the value of the downwash given by the table must be multiplied by 4, and the y of the table is obtained by adding 8 instead of 2 for a $0{\cdot}1$ interval, with an extra 5 for the interval $0{\cdot}9$ to $0{\cdot}9625$, amounting to $y = 93$ and 61 for the port and starboard half wings respectively. Row 6 then represents the individual contributions of unit rectangular vortices spaced along the span. The total contribution due to a given spanwise loading function is obtained by setting down the loading function as in row 5, which represents $\sqrt{(1-\eta^2)}$, and computing $\Sigma E\sqrt{(1-\eta^2)}$. The result is $0{\cdot}73342$, and after making allowance for factors which arise from the $\cot\frac{1}{2}\Theta$ function, and the non-dimensional form of the downwash Tables, the tangential flow relation gives for

$$\frac{kc}{8sV\sin\alpha} = a_0\sqrt{1-\eta^2}\cot\tfrac{1}{2}\Theta, \text{ the equation } 20a_0\,[0{\cdot}73342] = 1,$$

based on point 1, or, as usually written $0{\cdot}73342a_0 = 0{\cdot}05$. The formation of the complete equations is simply a matter of adding more functions and control points and proceeding in the same way, the right-hand side for the plane wing solution being $0{\cdot}05$ for all points. If the spacing were halved, giving 41 vortices, the method of procedure would be precisely the same, excepting that the right-hand side would be $0{\cdot}025$ instead of $0{\cdot}05$.

It is usually possible to arrange self-checking for most of the calculations. For example, in Table 2, row 3 can be checked by comparing the horizontal sum with the expression $40\Sigma a + 10\Sigma b$, and row 4 by comparing the horizontal sum with horizontal sum of row 3 less $21 \times 9{\cdot}550$. The integrals ΣE (load function) can be checked by comparing total sum of integrals with $\Sigma(\Sigma E)$ (Σ load functions).

6.2. We now describe the procedure for forming the equations for the 126-lattice. In Table 3, instead of the single row 3, we now have rows 2 to 7, which again represent the distances back from datum, and are obtained from Table 6 by taking $40a + 3{\cdot}3\dot{b}$, $40a + 10b$, and so on. In addition to these six, the distances back of the $\frac{1}{4}$-, $\frac{1}{2}$- and $\frac{3}{4}$-points are also given in rows 8, 9, 10 for a purpose which will be described below. In manuscript, the latter three are usually written in red to distinguish them from the other six. Now consider point 2 of Fig. 1, located at $\eta = 0{\cdot}2$ and $\frac{5}{6}$-chord, or $[0{\cdot}2, 10{\cdot}300]$. Rows 11 to 16 give the relative displacements of the individual vortices from the point 2, and it will be noted that the full lattice is only necessary for that part of the wing in the region of the control point, a reduction being made over the field beyond this. The simplification is introduced in order to save work in integration; for, beyond $y = 8$, there is very little loss in accuracy by taking the chordwise loading $\cot\frac{1}{2}\Theta$ as concentrated at the $\frac{1}{4}$-chord point, $\sin\Theta$ at the $\frac{1}{2}$-chord point, and $\sin 2\Theta$ as twin loads of opposite sign at the $\frac{1}{4}$- and $\frac{3}{4}$-chord points.

The downwash factors corresponding to the displacements are read from tables of downwash as before, and lead to an array of downwash factors of which three possible variations are given in rows 24 to 44 defined as 126/90, 126/86, and 126/74 respectively. The second number in each instance gives the total number of vortices used in integrating the downwash for a control point near the wing centre, when three chordwise terms are in use. With the chordwise terms limited to two, $\cot\frac{1}{2}\Theta$ and $\sin\Theta$, the E3 row beyond the centre lattice is omitted, and the numbers reduce to 78, 78, and 62 respectively.

The required load function, say $\sqrt{(1 - \eta^2)}$, is again put in row 23 and the preparation of the three downwash integrals, corresponding to $a_0 \cot \frac{1}{2}\Theta\sqrt{(1 - \eta^2)}$, $a_1 \sin \Theta\sqrt{(1 - \eta^2)}$, and $a_2 \sin 2\Theta\sqrt{(1 - \eta^2)}$ put in progress by the calculation of the nine integrals tabulated for the three solutions in rows 47 to 57. The first six of these integrals relate to the full centre lattice from 0·2 port to 0·6 starboard, while the other three cover the remainder of the lattice with the simplified chordwise representation. It should be noted that the last integral, which is obtained directly, is the difference $\Sigma E_1\sqrt{(1 - \eta^2)} - \Sigma E_3\sqrt{(1 - \eta^2)}$.

The first six integrals, therefore, give the downwash due to a load function $\sqrt{(1 - \eta^2)}$ on each of the six lines over the range $\eta = -0{\cdot}2$ to $+0{\cdot}6$, and the last three to $\sqrt{(1 - \eta^2)}$ over the remainder of the wing located on the $\frac{1}{4}$-chord, the $\frac{1}{2}$-chord, and the difference $\frac{1}{4}$-chord minus $\frac{3}{4}$-chord.

6.3. It is now necessary to consider the representation of a chordwise loading function. The method, based on two-dimensional reasoning, by which this is effected has been discussed in R. & M. 1910, where it is shown, for instance, that the distributed vorticity defined by $k = V \cot \frac{1}{2}\Theta$ can be represented by a vortex of strength $\frac{1}{2}\pi Vc$ placed at the $\frac{1}{4}$-chord, or, $0{\cdot}2734\pi Vc$, $0{\cdot}1172\pi Vc$, $0{\cdot}0703\pi Vc$, and $0{\cdot}0391\pi Vc$ placed at $\frac{1}{8}$-, $\frac{3}{8}$-, $\frac{5}{8}$-, and $\frac{7}{8}$-chord. The underlying idea is that, as the line vortices are to be used for the calculation of downwash at the midpoints of the lattice,the magnitudes should be such that the two-dimensional downwashes due to the line vortices, which follow from the geometry, are the same as for the distributed vorticity, which are usually known as mathematical functions. There is usually one fewer downwash relation than the number of line vortices, and the equations are completed by the stabilising condition that the total vorticity is correct.

It is assumed that the same relation holds when the flow is three-dimensional. Up to now the necessity has not arisen for any departure from this relation, the form of which would be inversely proportional to a function of aspect ratio, in order to give the correct limiting condition.

In addition to $\cot \frac{1}{2}\Theta$, similar factors for $\sin \Theta$ and $\sin 2\Theta$ for this and other vortex patterns have been obtained and are collected together in Table 7. A chordwise function, therefore, is represented by choosing the appropriate factors from Table 7 and applying them to the integrals of Table 3. For example, the coefficient of a_0, corresponding to $\cot \frac{1}{2}\Theta$, for the 126/90 solution is obtained by summing $0{\cdot}2256(47) + 0{\cdot}1025(48) + 0{\cdot}0684(49) + 0{\cdot}0488(50) + 0{\cdot}0342(51) + 0{\cdot}0205(52)$ for the centre part of the lattice and adding $0{\cdot}5(53)$ for the outer lattice; the coefficient of a_1, corresponding to $\sin \Theta$, by $0{\cdot}0273(47) + 0{\cdot}0456(48) + 0{\cdot}0521(49) + 0{\cdot}0521(50) + 0{\cdot}0456(51) + 0{\cdot}0273(52)$ for the centre lattice with $0{\cdot}25(54)$ added for the outer lattice; and the coefficient of a_2, corresponding to $\sin 2\Theta$, by $0{\cdot}0456(47) + 0{\cdot}0455(48) + 0{\cdot}0174(49) - 0{\cdot}0174(50) - 0{\cdot}0455(51) - 0{\cdot}0456(52)$ for the centre lattice with $0{\cdot}125(55)$ added for the outer lattice. After allowing for the factor, which is one half the vortex width in terms of the span, this gives for the tangential flow condition

$$0{\cdot}36011a_0 + 0{\cdot}21836a_1 + 0{\cdot}03113a_2 = 0{\cdot}025.$$

By adding further loading functions and control points the equations can be built up as required to the full number of variables.

6.4. It is again possible to arrange for most of the work to be self-checking. For example, the columns opposite rows 2 to 7 can be checked by comparing column sum with $240a + 120b$; a long column opposite rows 11 to 16 by comparing the sum with the sum of the column above less $61 \times 10{\cdot}300$; the integrals opposite rows 47 to 52, or 53 and 54, by comparing the sum with $\Sigma\,(\Sigma E)\sqrt{(1 - \eta^2)}$; the integrals in row 55 by comparing the sum of all such integrals with a total obtained directly from the chart; and the equations in the unknown variables by comparing horizontal sums with other values obtained directly from the integrals 47 to 55.

7. *Normalisation and Solution of Equations.*—If the number of equations exceeds the number of variables, it is necessary to normalise the equations before solution. The process is shown concisely for a hypothetical example in Table 8; further details can be obtained by reference to Whittaker and Robinson[3] or other standard works.

Assume that five relations are known in x_1 to x_3, x_4 being the unit root, or representing the constant column. The first normalised equation, row 6, is computed as follows:—$x_1 = \Sigma x_1^2$, $x_2 = \Sigma x_1 x_2$, $x_3 = \Sigma x_1 x_3$, $x_4 = \Sigma x_1 x_4$. The values $x_2 = \Sigma x_2^2$, $x_3 = \Sigma x_2 x_3$, $x_4 = \Sigma x_2 x_4$, are entered in row 7, and $x_3 = \Sigma x_3^2$ and $x_4 = \Sigma x_3 x_4$ in row 8, and the equations completed by making the square matrix x_1 to x_3 symmetrical about the diagonal. A check on the accuracy is obtained from the original equations by the following; $H_6 = \Sigma x_1 H_1$, $H_7 = \Sigma x_2 H_1$, $H_8 = \Sigma x_3 H_1$, where H_n is the horizontal sum of row n

The solution is carried out by elimination and proceeds in the order x_3, x_2, x_1, the constant column x_4 remaining until the end. The row with the greatest numerical value of x_3 is starred for elimination, which proceeds by the calculation of eliminating factors, for example $0{\cdot}42495$ being $6{\cdot}512/15{\cdot}324$. The work is continued by entering the quantity (row 6 $-$ $0{\cdot}42495$ row 8) in row 9—an immediate check on accuracy being made by comparing H_9 with $(H_6 - 0{\cdot}42495H_8)$ —and finishes at row 11, which gives $0{\cdot}168x_1 - 0{\cdot}245 = 0$. The remaining variables are evaluated by calculating the back solution, using in turn the starred rows, which give the greatest accuracy. A final check is applied by calculating the residuals due to substitution of the roots in the equations, in this case being practically zero to three places of decimals. The residuals for the original equations 1 to 5 have also been calculated in order to demonstrate the results to be expected in least squares solutions.

7.1. It is frequently necessary in connection with work on wing loading to vary the constant column, whilst leaving the remainder of the equations unchanged. The new solution can be found simply by following the procedure given at the lower part of Table 8, where a new x_4 column has been treated by the same eliminating factors as the original column. This leads directly to the revised relation $0{\cdot}168x_1 - 0{\cdot}222 = 0$, and the remaining roots are calculated from the back solution using the starred rows in the same way as previously.

8. *Calculation of Wing Characteristics.*—In order to demonstrate the means adopted to calculate some of the wing characteristics, a standard 126-vortex 6-point solution for the delta wing will be used. The equations for standard solution 3 of Fig. 4 and Table 22, obtained by the use of the 126/86-vortex layout as described in section 6, are given in Table 9. After solution of the equations, and calculation of $dC_L/d\alpha$ and yawing moment from relations (4) and (10), the work proceeds by the calculation of $F_0 + \frac{1}{2}F_1$, $F_0 + F_1 - \frac{1}{2}F_2$ (F_2 in this case being zero), and the position of the local aerodynamic centre on the chord

$$0{\cdot}25\,\frac{F_0 + F_1 - \frac{1}{2}F_2}{F_0 + \frac{1}{2}F_1}, \text{ for } \eta = 0(0{\cdot}05)1, \text{ where}$$

$$F_0 + \tfrac{1}{2}F_1 = 0{\cdot}11573\,\sqrt{(1-\eta^2)} - 0{\cdot}01590\eta^2\sqrt{(1-\eta^2)} - 0{\cdot}01022\eta^4\sqrt{(1-\eta^2)}$$

$$F_0 + F_1 - \tfrac{1}{2}F_2 = 0{\cdot}14029\,\sqrt{(1-\eta^2)} - 0{\cdot}09992\eta^2\sqrt{(1-\eta^2)} + 0{\cdot}06626\eta^4\sqrt{(1-\eta^2)}.$$

These calculations are given in Table 11, to which reference is now made. Column (5) gives the distance back, in terms of the span, of the local aerodynamic centre from datum, obtained from Table 10 by taking $[a + b \times$ column (4)$]$. Since column (2) is proportional to the wing loading, column (2) $\times$ column (5) is proportional to the moment of wing lift about the datum. Hence $\int$ column (6) divided by $\int$ column (2) gives the distance of the aerodynamic centre behind datum in terms of the span. The integrations are carried out by Simpson's Rule, and it should be noted that there is a variation from the usual factors near the tip, designed to make allowance

for the particular behaviour of the loading curve in this region (*see* Appendix V). The aerodynamic centre is at 0·5024 span or 1·160 mean chords behind the apex. The circulation $K/4sV$ is π (column (2)), and the local lift coefficient C_{LL} for unit C_L is calculated from 4π (column (2)) divided by $(c/2s \times (dC_L/d\alpha))$.

8.1. To find the effect of symmetrical linear wing twist, the equations are first converted to zero lift by using the condition $8a_0 + 4a_1 + 2c_0 + c_1 + e_0 + 0{\cdot}5e_1 + \ldots = 0$. The incidence equations of Table 9 are changed to the corresponding wing twist equations for solution 17 by the following conversions:—

a_0	Eliminated
a_1	$a_1 - 0{\cdot}5a_0$
c_0	$c_0 - 0{\cdot}25a_0$
c_1	$c_1 - 0{\cdot}125a_0$
e_0	$e_0 - 0{\cdot}125a_0$
e_1	$e_1 - 0{\cdot}0625a_0$.

Since the local geometrical incidence is now α_a + wing twist, the column for α_0 on the left-hand side becomes $-0{\cdot}025$ and the column for unit root $-0{\cdot}025$ (twist), which, for linear twist, is $-0{\cdot}025\eta$. The equations refer to one radian twist at the tip and the solution is given in Table 36. The calculations for c_{m0} and other quantities are shown in Table 12. The work proceeds exactly as for the aerodynamic centre calculations of Table 11, with the exception that c_{m0} is given by the expression

$$C_{m0} = -\frac{32\pi s^4}{S^2}\int_{-1}^{1} (\text{col. 6})\, d\eta = -\frac{64\pi s^4}{S^2}\int_{0}^{1} (\text{col. 6})\, d\eta = -\frac{64\pi s^4}{S^2}\,\frac{\Sigma(\text{col. 7})\ (\text{col. 6})}{60}$$

It will be noted that the local aerodynamic centre, given by column (4), is discontinuous at the point on the span where the circulation is zero. For a positive angle of twist and positive load at the tip, the local aerodynamic centre usually changes from $-\infty$ on the inner side to $+\infty$ on the outer side.

8.2. The solution for uniform roll is obtained exactly as for symmetrical wing twist, excepting that anti-symmetrical functions are used. The twist is taken as linear, and one radian at the tip corresponds to $V/\omega s = 1$.

8.3. Composite induced drags for standard solutions are calculated by working directly on the composite circulation. For example, a combination of solutions 3 and 17, representing incidence and wing twist for the delta wing, leads to the following formula for the circulation:—

$$K/4sV = \pi\,[(0{\cdot}11573\alpha_i - 0{\cdot}01306\alpha_t)\,\sqrt{(1-\eta^2)} + (-0{\cdot}01590\alpha_i + 0{\cdot}06842\alpha_t)\,\eta^2\sqrt{(1-\eta^2)} + (-0{\cdot}01022\alpha_i - 0{\cdot}03228\alpha_t)\,\eta^4\,\sqrt{(1-\eta^2)}]$$

where α_i and α_t are the incidence and angle of twist at the tip respectively. The formulae of Appendix I give

$$A_1 = \pi\,(0{\cdot}11048\alpha_i)$$
$$A_3 = \pi\,(-0{\cdot}00589\alpha_i + 0{\cdot}01105\alpha_t)$$
$$A_5 = \pi\,(-0{\cdot}00064\alpha_i - 0{\cdot}00202\alpha_t)$$

Hence
$$C_{Di} = \pi A \Sigma n A_n^2$$
$$= \pi^3 A\,(0{\cdot}01231\alpha_i^2 - 0{\cdot}00038\alpha_i\alpha_t + 0{\cdot}00039\alpha_t^2)$$

For a given incidence α_i, the induced drag is a minimum when,

$$0{\cdot}00078\alpha_t - 0{\cdot}00038\alpha_i = 0 \text{ or } \alpha_t = 0{\cdot}4872\alpha_i, \text{ giving } \pi A\ (0{\cdot}01222\alpha_i^2),$$
the absolute minimum being $\pi A\ (0{\cdot}11048)^2\alpha_i^2$ or $\pi A\ (0{\cdot}01221\alpha_i^2)$.

9. *Solutions for Delta Wing.*—Fifteen solutions are given for incidence for a delta wing, equilateral triangle, and seven solutions for twist, with angle of twist linear. The former are given in Tables 20 to 34 and Figs. 4 to 7 and the latter in Tables 35 to 41 and Figs. 4 to 7. The solutions range from 21-vortex to 328-vortex, and all the necessary information as to the derivation of the solutions can be obtained from the tables and figures. Where more control points than variables are shown, the equations have been reduced by normalisation before solution. We proceed directly to enumerate the solutions.

9.1. *Incidence Solutions.*—The first part of the work is connected with standard solutions, and is concerned mainly with the effects of alteration of the number of control points and the spacing of the lattice. The two 21-vortex solutions 1 and 2 given in Fig. 4 and Tables 20 and 21 demonstrate that three stations are sufficient to give good accuracy in the spanwise direction, the addition of two extra stations making no appreciable difference. The succeeding solutions 3 to 6, given in Figs. 4 and 5, and Tables 22 to 25, show (a) that there is no appreciable difference between the results for 6- and 9-points used with the 126-vortex lattice, (b) that the 9- and 12-point solutions with the 328-vortex lattice are in good agreement and (c) that the 126-vortex 6-point solution agrees quite well, except for the value of $dc_L/d\alpha$, with the 328-vortex 12-point solution. From this we conclude that the validity of the 126-vortex 6-point solution for general use as the standard solution is established, the only correction required being to apply a factor to the value of $dc_L/d\alpha$.

These solutions have been treated in a general manner and do not include a special condition applicable to a pointed tip. This extra condition is that the local aerodynamic centre at the tip is at $\frac{1}{4}$-chord, which must apply if the reasonable assumption be made that the curvature of flow at the tip remains finite. The effect of this condition is negligible as far as the wing loading is concerned, the main effect being to improve the curve of local aerodynamic centre plotted against η. An example of the application of the condition will be given below.

9.1.1. It is now necessary to consider what modifications are required to the standard solution in order to allow for the effect of sudden change of direction of the leading or trailing edge. That a modification is necessary can easily be demonstrated by forming more equations for the standard solution in the region of the discontinuity, when it will be found that they are not satisfied by the standard solution. The discrepancy is worst at the discontinuity, which can be seen from Table 13, in which the standard equations for points 7 to 10 (*see* Fig. 6), have been set down for the 126-vortex solution. The residuals after substitution of solution 3 are given in the last column; they are greatest at the discontinuity and drop to about one-fifth the value at $0{\cdot}1$ semispan or one vortex width away from the discontinuity.

It is obvious from the standard calculations that the effect of the discontinuity must be small at distances away of $0{\cdot}2\eta$ or greater, and the necessity for easy calculation of induced drag and yawing moment leads us to the use of the P functions as mentioned in section 2. We require an additional circulation function of which the corresponding distribution of w/V has a peak at the discontinuity, and, if the argument be limited to two additional spanwise terms suitable combinations of the P functions for the delta wing are P_a and P_b as shown in Fig. 8. These functions are formed by addition of proportions of the P functions as indicated in Ref. 7, the formula being

$$P_a = \sqrt{(1 - \eta^2)} - 10P_{s00} + 9P_{s10}$$
$$P_b = \sqrt{(1 - \eta^2)} - 5P_{s00} + 4P_{s20}.$$

As the $0{\cdot}1$ lattice in effect limits us to intervals of $0{\cdot}1s$, and it is known that w/V should become negligible at $\eta = 0{\cdot}2$ or slightly greater, no other reasonable choice is available.

9.1.2. As the use of both P_a and P_b implies to 10-point solution, the procedure is to reduce to a single variable P which is a combination of P_a and P_b. This is effected by a subsidiary calculation involving the six points 1, 2, 7, 8, 9, 10 only. We require to find an additional solution which will remove the discrepancies noted in the standard solution. It is, therefore, assumed that the formula for $kc/8sV \sin \alpha$ is precisely as for the standard solution, relation (2), but with the following additions:—

$$\text{To } F_0 \text{ add } a_0'\sqrt{1-\eta^2} + p_{a0}P_a + p_{b0}P_b \quad .. \quad .. \quad .. \quad .. \quad .. \quad (14)$$

$$\text{To } F_1 \text{ add } a_1'\sqrt{1-\eta^2} + p_{a1}P_a + p_{b1}P_b. \quad .. \quad .. \quad .. \quad .. \quad .. \quad (15)$$

The terms in a_0' and a_1' are found to be necessary in order to balance the terms in P.

The additional loading functions are treated in the same way as the standard loading functions and lead to the equations of Table 15 for the six points 1, 2, 7, 8, 9, 10. In order that the downwash due to the six terms of these equations shall remove the discrepancies in the standard solution, the constant column must be the same as the residuals obtained from Table 13, those for the additional points 1 and 2, two of the standard equating points, being zero.

9.1.3. The values of the extra functions P_a and P_b together with combinations of the two are given in Table 46, and are plotted with the corresponding downwash distribution in Fig. 8. It will be noted that two sets of values are given, the first the true values, and the second special values to be used with the 0·1 lattice. A full explanation of the derivation of the two sets is given in Appendix VII.

9.1.4. The equations of Table 15 are representative of general practice when the discontinuity is at $\eta = 0$. When the trailing edge is straight as in the case of the delta wing, it appears that the rounding-off effect of the discontinuity is mainly reflected in movement of the local aerodynamic centre, the circulation remaining almost unchanged. This effect will be demonstrated below, but, if the fact be accepted, the equations of Table 15 can be simplified by using the conditions that the circulation is unaltered, *i.e.*,

$$a_0' + \tfrac{1}{2}a_1' = p_{a0} + \tfrac{1}{2}p_{a1} = p_{b0} + \tfrac{1}{2}p_{b1} = 0$$

The simplified equations are given in Table 17, and the solution in Table 26. As the solution is intended only to round-off the standard solution, the revised figures for local aerodynamic centre are used only as far as the point, in this case $\eta = 0{\cdot}5$, where the new curve merges into the original, after which the original curve is followed.

The ratio of p_{a0} to p_{b0} is of the order 0·6 to 0·4, and, as the final answer is not very sensitive to this ratio, the most useful combination of functions, having regard to other uses as well, is taken to be $P = 0{\cdot}65P_a + 0{\cdot}35P_b$. The values of this function are given in Table 46, and are plotted with the corresponding downwash distribution in Fig. 8.

9.1.5. The rounding-off equations can now be simplified by using the following additions:—

$$\text{to } F_0 \text{ add } a_0'\sqrt{(1-\eta^2)} + p_0P$$

$$\text{to } F_1 \text{ add } a_1'\sqrt{(1-\eta^2)} + p_1P,$$

which, after use of the conditions for unchanged circulation,

$$a_0' + \tfrac{1}{2}a_1' = p_0 + \tfrac{1}{2}p_1 = 0$$

lead to the four equations of Table 18 for the points 1, 2, 7, 8 in the two variables a_0' and p_0. The solution of these equations is given in Table 27. Again the values of $K/4sV$ and C_{LL} correspond to those of solution 3, and the modified local aerodynamic centre is followed up to $\eta = 0{\cdot}5$ only. The position of the overall aerodynamic centre for solution 8 is at $1{\cdot}183\bar{c}$ behind the apex, *i.e.*, it is at $0{\cdot}023\bar{c}$ farther back than the standard solution.

For the general case represented by solutions 14 and 15, the additional lift is

$$dC_L/d\alpha = \tfrac{1}{2}\frac{\pi^2 S^2}{S}[8\,(a_0' + \tfrac{1}{2}a_1') + 0{\cdot}50888\,(p_{a0} + \tfrac{1}{2}p_{a1}) + 1{\cdot}01517\,(p_{b0} + \tfrac{1}{2}p_{b1})].$$

9.1.6. The form of the additional loading function being fixed, it is now possible to make a complete revision of the standard solutions by solving a range of solutions up to 8 points. The work is started by solving a 21-vortex 4-point solution with one control point at $\eta = 0$, and including in the loading functions the given function P. This solution, number 9, is given in Table 28, and, by the practical rejection of the term in p_0, provides additional confirmation that the standard terms are adequate for a satisfactory solution.

This is followed by an 8-point solution, number 10, in which points 7 and 8 are added to the standard solution, and terms p_0 and p_1 to the standard loading functions. The value of $p_0 + \frac{1}{2}p_1$ has the small value of 0·00538, confirming that the main effect of the rounding-off at the discontinuity is to shift back the local aerodynamic centre.

Solution 11 has been calculated in order to show the effect of reducing the lattice from the 126/86 to 126/74 pattern (Table 3). The difference in the results is not great, but, in the opinion of the computers who carried out the work, the simplification is not worth while. Solution 12 has been calculated with the same number of variables but with the addition of two extra control points located at $\eta = 0{\cdot}7$. The difference between the two solutions is very small and so provides additional evidence of the accuracy of the eight-point solutions. Solution 13 is the same as solution 10, but with the condition that the P functions alter the local aerodynamic centre only and add nothing to the loading functions, *i.e.*, $p_0 + \frac{1}{2}p_1 = 0$. This leads to seven independent variables only, and, after normalisation and solution of the equations, the solution given in Table 32 is obtained. There is very little difference between this and solution 10, and, although no exact proof of the condition has been given, it is at least evident that it is correct for all practical purposes.

9.1.7. To end the series of incidence solutions, solution 14 has been computed with the additional condition that the local aerodynamic centre at the wing tip is at $\frac{1}{4}$-chord. This is a special condition for pointed tips and it leads to a relation between a_1, c_1, e_1, and p_1 derived in the following way. For $\eta = 1$, $(F_0 + F_1 - \frac{1}{2}F_2) / (F_0 + \frac{1}{2}F_1)$ must be unity. Cancelling the factor $\sqrt{(1 - \eta^2)}$, we are left with

$$a_1 + c_1 + e_1 + p_1\left(\frac{P}{\sqrt{(1-\eta^2)}}\right)_{\eta=1} = 0,$$

or since $P/\sqrt{(1 - \eta^2)} = T_{20}$, we have from Table 46,

$$a_1 + c_1 + e_1 + 0{\cdot}04303p_1 = 0.$$

The solution, although based on six independent variables only, does not differ greatly from number 10, but the curve of local aerodynamic centre is perhaps the most accurate of any for the delta wing.

Finally, the lifting-line solution has been calculated by standard methods and is given for comparison as solution 15.

9.2. *Wing Twist Solutions.*—Seven solutions applicable to linear wing twist are given in Tables 35 to 41. Solution 16 is the 21-vortex 3-variable standard solution, and is followed by solution 17, a 126-vortex 6-point standard solution and solution 18, a 328-vortex 12-point standard solution. These three solutions have been calculated in order to provide evidence as to the accuracy of the standard solutions and they show at once that the spanwise stations used are sufficient for an accurate estimate of the circulation. The 21-vortex solution, however, should be avoided, if an accurate estimate of C_{m0} is required, for it is evident that departures from the $\frac{1}{4}$-chord position for the local aerodynamic centre are very much more important for twist solutions than for incidence solutions.

9.2.1. The rounding-off effect of the discontinuity is again assessed by methods similar to those used for the incidence solutions. Solution 19 involves the six points 1, 2, 7, 8, 9, 10 of Fig. 6. The additional standard equations for linear wing twist for the points 7, 8, 9, and 10 are given in Table 14, together with the residuals after substitution of the standard solution 17. The auxiliary equations are found to be entirely satisfactory if the same additional variables as before are used, *i.e.*, a_0', a_1', p_{a0}, p_{a1}, p_{b0}, p_{b1}. In order to transform to the equations applicable to zero lift, the zero lift condition relating to the new variables only is used, *i.e.*, $8a_0' + 4a_1' + 0{\cdot}50888p_{a0} + 0{\cdot}25444p_{a1} + 1{\cdot}01517p_{b0} + 0{\cdot}50758p_{b1} = 0$.

9.2.2. The equations are given in Table 16 and the solution in Table 38. It as apparent from this that a suitable ratio between the two functions is $(p_{a0} + \frac{1}{2}p_{a1})$ to $(p_{b0} + \frac{1}{2}p_{b1})$ or 0·250 to 0·750. The solution is not very sensitive to this ratio and the combined function actually used was $0{\cdot}2P_a + 0{\cdot}8P_b$ the values being given in Table 46 and Fig. 8. Using this function, a simplified auxiliary solution number 20, using the six points, with equations given in Table 19, was also calculated. Finally, the full eight point solution using the eight points 1 to 8 and with $P = 0{\cdot}2P_a + 0{\cdot}8P_b$ added to the standard loading functions has been calculated and is given as solution 21, Table 40.

Finally the lifting-line solution is given in Table 41. A four point rounding-off solution for points 1, 2, 7, 8 has not been calculated but there is little doubt that this would be entirely satisfactory.

9.3. *Discussion of Results: Incidence Solutions.*—In Fig. 9, solutions 3 and 4 have been plotted in order to demonstrate how close is the agreement between 126-vortex 6-point and 9-point solutions. Similarly, in Fig. 10, two 328-vortex solutions with 9 and 12 points respectively have been plotted and also show close agreement. Figure 11 is concerned with the effect of the rounding-off terms on the 126-vortex solutions and includes the standard solution No. 3, an 8-point unconditional solution number 10, an 8-point conditional solution number 14, and a quick modification to the standard solution, number 8. Finally, in Figure 12, solutions of varying complexity are compared. The loci of the local aerodynamic centre for lifting line, standard and modified solutions are shown in Fig. 15.

A summary of the main characteristics of the incidence solutions is given in Table 42.

9.3.1. The following conclusions are drawn after a study of these solutions:—

(a) The spanwise distribution of local lift coefficient is in close agreement for all vortex lattice solutions. This conclusion is valid for wings with straight trailing edges, but judgment is reserved on the question whether the 21-vortex solutions will be equally accurate when a sweptback trailing edge is involved. The 21-vortex solutions are valuable for establishing the circulation and for the determination of the functions to be used for any particular problem. The lifting-line solution is greatly in error.

(b) When the local or overall aerodynamic centres are required the 21-vortex solutions are not sufficiently accurate.

(c) The 126-vortex 6-point solution is established as sufficient to give good accuracy for the standard solution. The only appreciable error (*see* Table 42) is in $dc_L/d\alpha$, which, if solution 6 be accepted as the most accurate, must be increased by the factor 1·038. Similarly, $dc_L/d\alpha$ for the 21-vortex solution number 1, must be increased by the factor 1·088.

These corrections are in addition to these due to the rounding-off effects on the lift of discontinuities, which, although negligible for this wing, may be quite appreciable when sweepback of the trailing edge is present.

(d) For the delta wing, and probably for any wing with a straight trailing edge, the effect of the rounding-off due to the discontinuity, which is not allowed for in the standard solution,

is to shift backwards the local aerodynamic centre in the region of the discontinuity, and to leave the circulation and $dc_L/d\alpha$ practically unchanged. The overall shift backwards of the aerodynamic centre is about $0{\cdot}020\bar{c}$. When the trailing edge is not straight there will be an additional effect of change of circulation.

(e) The additional loading functions necessary to allow for the discontinuity can easily be built up from special functions given in another report. After a single combined function has been established, the full modification to the 126-vortex solution involves an 8-point solution the extra two points being located at the discontinuity. It is shown that the necessary modification can be effected with good accuracy when the combined function is known by an auxiliary solution involving only four variables generally and two for those cases where the circulation is unchanged. If the combined function is not known, the additional work required need not be great. As evidence of this conclusion, the simple solution number 8 agrees very well with the 8-point solution number 10.

(f) The auxiliary functions required are remarkably consistent and it will be possible later to predict those required for any problem.

9.4. *Discussion of Results: Wing Twist Solutions.*—Selections from the solutions for wing twist are plotted in Figs. 13 and 14. In Fig. 13 the three standard solutions of 21, 126 and 328 vortices respectively are plotted and the agreement between the latter two shows again that the 126-vortex 6-point solution is adequate for obtaining an accurate standard solution.

Selections from the solutions after allowance for the effect of the discontinuity are plotted in Fig. 14. Loci of the local aerodynamic centre for lifting line and other solutions are shown in Fig. 15. A summary of the twist solutions is given in Table 43.

9.4.1. The following conclusions are derived from a study of these results:—

(a) The spanwise distributions of circulation per radian twist are in agreement for the three standard solutions, but the use of the 21-vortex solution may be invalidated on account of the large error in c_{m0}. There is good agreement in all respects between the 126- and 328-vortex solutions, from which it is deduced that the 126-vortex 6-point solution will give an accurate standard solution.

(b) For the delta wing—and it is not yet known whether this result is general—the effect of allowing for the discontinuity at the median section is to leave the local centres of pressure unaltered but to increase the circulation per radian twist. This effect is the reverse to that experienced with the incidence solutions.

(c) The additional loading functions necessary to allow for the discontinuity are built up from the standard functions of Ref. 7 in the same way as for incidence solutions. A solution with accuracy almost equal to a full 8-point solution can be obtained by a simple auxiliary solution as in the case of incidence solutions.

(d) For the delta wing—and again, generality cannot be assumed—an approximate correction to the standard solution can be obtained by multiplying $K/4sV$ and c_{m0} by a factor, of the order of $1{\cdot}06$.

(e) The lifting-line solution is subject to serious errors, c_{m0}, for instance, being about 50 per cent in excess of the vortex lattice values.

10. *Acknowledgements.*—The writer wishes to acknowledge his indebtedness to Messrs. H. B. Squire and M. Gdaliahu who pointed out the application of Munk's Stagger Theorem, without which the calculation of induced drag would be exceedingly difficult; to Miss S. W. Skan, for valuable assistance in establishing the standard method of normalisation and solution of equations; and to Misses S. D. Brown, P. I. Bond and W. M. Tafe for bearing the responsibility of computing and checking the calculations on which the report is based.

11. *Conclusion.*—This report has demonstrated the general principles of the use of vortex-lattice theory for the special case of the delta wing. Examples of application to wings with large sweepback, including the special methods to be adopted for the general determination of induced drag and yawing moment, will be dealt with in a later report.

APPENDIX I

Relation Between Lifting-line and Lifting-plane Notation

The Glauert or lifting-line notation is

$$\frac{K}{4sV \sin \alpha} = \sum_{n=1}^{\infty} A_n \sin n\phi$$

and the corresponding lifting-plane notation is

$$\begin{aligned}\frac{K}{4sV \sin \alpha} &= \pi \left[(F_0 + \tfrac{1}{2}F_1)\right.\\ &= \pi \left[(a_0 + \tfrac{1}{2}a_1)\sqrt{(1-\eta^2)} + (b_0 + \tfrac{1}{2}b_1)\,\eta\sqrt{(1-\eta^2)} + (c_0 + \tfrac{1}{2}c_1)\right.\\ &\qquad \left.\eta^2\sqrt{(1-\eta^2)} + \ldots\ldots + (k_0 + \tfrac{1}{2}k_1)\,\eta^{10}\sqrt{(1-\eta^2)} + \ldots\ldots\right]\end{aligned}$$

Since $\eta = \cos\phi$, standard formulae give (Hobson p. 106)[8]

$$\begin{aligned}
\sin\phi &= \sqrt{1-\eta^2}\\
\sin 2\phi &= 2\eta\sqrt{1-\eta^2}\\
\sin 3\phi &= \sqrt{1-\eta^2}\,(4\eta^2 - 1)\\
\sin 4\phi &= \sqrt{1-\eta^2}\,(8\eta^3 - 4\eta)\\
\sin 5\phi &= \sqrt{1-\eta^2}\,(16\eta^4 - 12\eta^2 + 1)\\
\sin 6\phi &= \sqrt{1-\eta^2}\,(32\eta^5 - 32\eta^3 + 6\eta)\\
\sin 7\phi &= \sqrt{1-\eta^2}\,(64\eta^6 - 80\eta^4 + 24\eta^2 - 1)\\
\sin 8\phi &= \sqrt{1-\eta^2}\,(128\eta^7 - 192\eta^5 + 80\eta^3 - 8\eta)\\
\sin 9\phi &= \sqrt{1-\eta^2}\,(256\eta^8 - 448\eta^6 + 240\eta^4 - 40\eta^2 + 1)\\
\sin 10\phi &= \sqrt{1-\eta^2}\,(512\eta^9 - 1024\eta^7 + 672\eta^5 - 160\eta^3 + 10\eta)\\
\sin 11\phi &= \sqrt{1-\eta^2}\,(1024\eta^{10} - 2304\eta^8 + 1792\eta^6 - 560\eta^4 + 60\eta^2 - 1).
\end{aligned}$$

Equating the two expressions gives the following:—

$$\begin{aligned}
A_1 &= \pi[a_0 + \tfrac{1}{2}a_1 + \tfrac{1}{4}c_0 + \tfrac{1}{8}c_1 + \tfrac{1}{8}e_0 + \tfrac{1}{16}e_1 + \tfrac{5}{64}g_0 + \tfrac{5}{128}g_1 + \tfrac{7}{128}i_0 + \tfrac{7}{256}i_1 + \tfrac{21}{512}k_0\\
&\qquad + \tfrac{21}{1024}k_1]\\
A_2 &= \pi\,[\tfrac{1}{2}b_0 + \tfrac{1}{4}b_1 + \tfrac{1}{4}d_0 + \tfrac{1}{8}d_1 + \tfrac{5}{32}f_0 + \tfrac{5}{64}f_1 + \tfrac{7}{64}h_0 + \tfrac{7}{128}h_1 + \tfrac{21}{256}j_0 + \tfrac{21}{512}j_1]\\
A_3 &= \pi\,[\tfrac{1}{4}c_0 + \tfrac{1}{8}c_1 + \tfrac{3}{16}e_0 + \tfrac{3}{32}e_1 + \tfrac{9}{64}g_0 + \tfrac{9}{28}g_1 + \tfrac{7}{64}i_0 + \tfrac{7}{128}i_1 + \tfrac{45}{512}k_0 + \tfrac{45}{1024}k_1]\\
A_4 &= \pi\,[\tfrac{1}{8}d_0 + \tfrac{1}{16}d_1 + \tfrac{1}{8}f_0 + \tfrac{1}{16}f_1 + \tfrac{7}{64}h_0 + \tfrac{7}{128}h_1 + \tfrac{3}{32}j_0 + \tfrac{3}{64}j_1]
\end{aligned}$$

$$A_5 = \pi\,[\tfrac{1}{16}e_0 + \tfrac{1}{32}e_1 + \tfrac{5}{64}g_0 + \tfrac{5}{128}g_1 + \tfrac{5}{64}i_0 + \tfrac{5}{128}i_1 + \tfrac{75}{1024}k_0 + \tfrac{75}{2048}k_1]$$
$$A_6 = \pi\,[\tfrac{1}{32}f_0 + \tfrac{1}{64}f_1 + \tfrac{3}{64}h_0 + \tfrac{3}{128}h_1 + \tfrac{27}{512}j_0 + \tfrac{27}{1024}j_1]$$
$$A_7 = \pi\,[\tfrac{1}{64}g_0 + \tfrac{1}{128}g_1 + \tfrac{7}{256}i_0 + \tfrac{7}{512}i_1 + \tfrac{35}{1024}k_0 + \tfrac{35}{2048}k_1]$$
$$A_8 = \pi\,[\tfrac{1}{128}h_0 + \tfrac{1}{256}h_1 + \tfrac{1}{64}j_0 + \tfrac{1}{128}j_1]$$
$$A_9 = \pi\,[\tfrac{1}{256}i_0 + \tfrac{1}{512}i_1 + \tfrac{9}{1024}k_0 + \tfrac{9}{2048}k_1]$$
$$A_{10} = \pi\,[\tfrac{1}{512}j_0 + \tfrac{1}{1024}j_1]$$
$$A_{11} = \pi\,[\tfrac{1}{1024}k_0 + \tfrac{1}{2048}k_1].$$

The following are the relations between ϕ and η :—

$$\sqrt{(1-\eta^2)} = \sin\phi$$
$$\eta\sqrt{(1-\eta^2)} = \tfrac{1}{2}\sin 2\phi$$
$$\eta^2\sqrt{(1-\eta^2)} = \tfrac{1}{4}(\sin\phi + \sin 3\phi)$$
$$\eta^3\sqrt{(1-\eta^2)} = \tfrac{1}{8}(2\sin 2\phi + \sin 4\phi)$$
$$\eta^4\sqrt{(1-\eta^2)} = \tfrac{1}{16}(2\sin\phi + 3\sin 3\phi + \sin 5\phi)$$
$$\eta^5\sqrt{(1-\eta^2)} = \tfrac{1}{32}(5\sin 2\phi + 4\sin 4\phi + \sin 6\phi)$$
$$\eta^6\sqrt{(1-\eta^2)} = \tfrac{1}{64}(5\sin\phi + 9\sin 3\phi + 5\sin 5\phi + \sin 7\phi)$$
$$\eta^7\sqrt{(1-\eta^2)} = \tfrac{1}{128}(14\sin 2\phi + 14\sin 4\phi + 6\sin 6\phi + \sin 8\phi)$$
$$\eta^8\sqrt{(1-\eta^2)} = \tfrac{1}{256}(14\sin\phi + 28\sin 3\phi + 20\sin 5\phi + 7\sin 7\phi + \sin 9\phi)$$
$$\eta^9\sqrt{(1-\eta^2)} = \tfrac{1}{512}(42\sin 2\phi + 48\sin 4\phi + 27\sin 6\phi + 8\sin 8\phi + \sin 10\phi)$$
$$\eta^{10}\sqrt{(1-\eta^2)} = \tfrac{1}{1024}(42\sin\phi + 90\sin 3\phi + 75\sin 5\phi + 35\sin 7\phi + 9\sin 9\phi + \sin 11\phi).$$

APPENDIX II

Calculation of Lift Coefficient: Standard Solution

$$\frac{kc}{8sV\sin\alpha} = F_0\cot\tfrac{1}{2}\Theta + F_1\sin\Theta + F_2\sin 2\Theta$$

The circulation $K = \int_{-c/2}^{c/2} k\,dx$

or $$\frac{K}{8sV\sin\alpha} = \frac{F_0}{c}\int_{-c/2}^{c/2}\cot\tfrac{1}{2}\Theta\,dx + \frac{F_1}{c}\int_{-c/2}^{c/2}\sin\Theta\,dx + \frac{F_2}{c}\int_{-c/2}^{c/2}\sin 2\Theta\,dx.$$

But $x/c = \tfrac{1}{2}\cos\Theta$, therefore $(1/c)\int_{-c/2}^{c/2}\cot\tfrac{1}{2}\Theta\,dx = \tfrac{1}{2}\int_0^{\pi}\cot\tfrac{1}{2}\Theta\sin\Theta\,d\Theta = \pi/2.$

Similarly, $(1/c)\int_{-c/2}^{c/2}\sin\Theta\,dx = \pi/4$ and $(1/c)\int_{-c/2}^{c/2}\sin 2\Theta\,dx = 0.$

Hence $\frac{K}{4sV\sin\alpha}$ or $\frac{K}{4sV}$ per radian $= \pi\,(F_0 + \tfrac{1}{2}F_1)$.

The element of lift on any chord is $\rho VK\,dy$, or total lift $= \int_{-s}^{s} \rho VK\,dy$.

Hence, $\frac{c_L}{\sin\alpha}$ or $\frac{dc_L}{d\alpha} = \frac{2s}{VS}\int_{-1}^{1} K\,d\eta = \frac{8\pi s^2}{S}\int_{-1}^{1} (F_0 + \frac{1}{2}F_1)\,d\eta$.

After substitution of the integrals (*see* Table 5), this becomes

$$\frac{c_L}{\sin\alpha} \text{ or } \frac{dc_L}{d\alpha} = \frac{\pi^2 s^2}{2S}\,(8a_0 + 4a_1 + 2c_0 + c_1 + e_0 + 0{\cdot}5e_1 + 0{\cdot}625g_0 + 0{\cdot}03125g_1 + 0{\cdot}4375i_0 + 0{\cdot}21875i_1 + 0{\cdot}328125k_0 + 0{\cdot}1640625k_1).$$

This formula is independent of the shape of the wing.

APPENDIX III

Calculation of Local Lift Coefficient

The local lift coefficient $c_{LL} = \frac{\rho VK}{\frac{1}{2}\rho V^2 c} = \frac{8\pi s}{c}\sin\alpha\,(F_0 + \frac{1}{2}F_1)$. At the median section where $\eta = 0$, $F_0 = a_0$, $F_1 = a_1$, and $c_{LL} = \frac{8\pi s}{c}\sin\alpha\,(a_0 + \frac{1}{2}a_1)$.

The local lift coefficient at the tip, when this is rounded-off by a circle of radius R, is calculated as follows. At a distance of $d\eta$ from the tip, $c/s = \sqrt{(8Rd\eta/s.)}$.

Also, as $\eta \to 1$, $\sqrt{1-\eta^2} \to \sqrt{[1-(1-d\eta)^2]}$, and

$$c_{LL} = \frac{8\pi s}{c}\sin\alpha\,\sqrt{[1-(1-d\eta)^2]}\,[a_0 + \tfrac{1}{2}a_1 + (b_0 + \tfrac{1}{2}b_1)\,\eta + (c_0 + \tfrac{1}{2}c_1)\,\eta^2 + \ldots.].$$

Hence, at the tip, where $\eta = 1$,

$$c_{LL} = 4\pi\sqrt{\left(\frac{s}{R}\right)}\sin\alpha\,[a_0 + \tfrac{1}{2}a_1 + b_0 + \tfrac{1}{2}b_1 + c_0 + \tfrac{1}{2}c_1 + \ldots\ldots.].$$

APPENDIX IV

Calculation of Yawing Moments by Lifting-Line Theory

Yawing moments are due to two factors, (a) the effect of the symmetrical downwash on the anti-symmetrical loading and (b) the effect of anti-symmetrical downwash on the symmetrical loading.

For the lifting-line loading per radian

$$K/4sV = \Sigma A_n \sin n\phi,$$

the yawing moment is $N = \int_{-s}^{s} \rho w K s \cos\phi \, dy,$

and $$c_n = \frac{1}{\rho V^2 s S} \int_{-s}^{s} \rho w K s \cos\phi \, dy$$

$$= \frac{4s^2}{S} \int_0^{\pi} \cos\phi \, \Sigma A_n \sin n\phi \, \Sigma n A_n \sin n\phi \, d\phi$$

from which the following value for the yawing moment coefficient is derived

$$C_n = \frac{\pi s^2}{S} [3A_1A_2 + 5A_2A_3 + 7A_3A_4 + \ldots\ldots + (2n+1) A_nA_{n+1} + \ldots\ldots].$$

APPENDIX V

On a Modification to Simpson's Factors

The Simpson factors 1, 4, 1, are based on the assumption that the curve through three points can be represented by $y = ax + bx^2$. If dy/dx is infinite, this assumption is invalid, and the use of the factors 1, 4, 1, leads to errors in the integration.

The Simpson factors can be modified to allow for dy/dx being infinite in the following way:—let the three ordinates be y_0, y_1, y_2, where dy/dx is infinite at $y = y_0$. Let $y = K_0 + K_1x^{1/2} + K_2x^{3/2}$ and hence

$$\frac{dy}{dx} = \tfrac{1}{2}K_1x^{-1/2} + \tfrac{3}{2}K_2x^{1/2}.$$

The area is $\int_0^x y\,dx = K_0x_2 + \tfrac{2}{3}K_1x_2^{3/2} + \tfrac{2}{5}K_2x_2^{5/2}$

Let the area be $\frac{1}{6}(a_0y_0 + a_1y_1 + a_2y_2)\, x_2$ where $a_0 + a_1 + a_2 = 6$. Substituting for y_0, y_1 and y_2, and noting that $x_1 = \frac{1}{2}x_2$, the solution of the equality gives $a_0 = 0{\cdot}675$, $a_1 = 4{\cdot}525$, $a_2 = 0{\cdot}800$ which take the place of 1, 4, 1, the value a_0 being used at the point where dy/dx is infinite.

The following table is an example of the integration of $\sqrt{(1 - x^2)}\, dx$ from $x = 0$ to 1. The true integral is $\pi/4$ or $0{\cdot}7854$ and the superiority of the modified formula is clearly demonstrated. Professor Bickley[5] has pointed out that the use of these factors is only justified when the conditions at the vertical slope are in agreement with the assumptions made, and has generalised the analysis to suit a varying range of tip conditions.

x	$\sqrt{(1-x^2)}$	Simpson factors	Modified Simpson factors
0	1·0000	1	1
0·1	0·9950	4	4
0·2	0·9798	2	2
0·3	0·9539	4	4
0·4	0·9165	2	2
0·5	0·8660	4	4
0·6	0·8000	2	2
0·7	0·7141	4	4
0·8	0·6000	2	1·800
0·9	0·4359	4	4·525
1·0	0	1	0·675

Integral	Value
True	0·7854
Simpson	0·7817
Simpson modified	0·7854

APPENDIX VI

Tables of Complete Downwash for a Rectangular Vortex

The tables of complete downwash are constructed from the formulae published by Glauert[6], and given in Fig. 3. The origin and location point of the vortex is the midpoint of the bound vortex AA′, and the non-dimensional co-ordinates are $x^* = x/y_v$, positive forwards, and $y^* = y/y_v$, positive towards the starboard side, where y_v is the semi-width of the vortex.

The function tabulated is the total downwash $2\pi w/V$ for three line vortices AA′, AB, and A′B′, each of strength $K = 2Vy_v$. The tables are constructed for specified values of y^*, with x^* as the running co-ordinate, the configuration of the lattice making it necessary to include only the sequences $y^* = 2(2)88$, and $13(8)173$. For $y^* = 0$, the function becomes infinite as $x^* \to 0$, and, in this region, the tables would be unsuitable for interpolation or for being converted to a critical form. On the recommendation of the Scientific Computing Service Ltd., the tables for $y^* = 0$ with x^* small have, therefore, been modified by tabulating the complete downwash less a part $2/x^*$, an artifice which removes the infinity and restores the tables to a readily usable form.

Straight tables derived from key tables computed by the Scientific Computing Service Ltd., and critical tables derived by interpolation from the straight tables, have previously been used and circulated. As the use of the tables is now firmly established, it has been considered well worth the expense of having the critical tables recomputed to greater accuracy and consistency. This work has been undertaken by the Mathematics Division of the Laboratory, and the tables are now to be published as a separate report.[4] They were computed by a direct process, Glauert's formula for w in terms of x^*, y^* being inverted analytically to give x^* in terms of w and y^*.

The opportunity has been taken of simplifying the use of those tables for the series $y^* = 13(8)173$, which are associated with the corrector vortices and will be referred to as subsidiary Tables, by tabulating four times the downwash against $\frac{1}{4}x^*$. It should be noted that the stars have been omitted in the latest Tables.

APPENDIX VII

Variations of Functions in Accordance with Their Uses

It is convenient as well as reasonable to use lifting-line theory as a measure of the accuracy of the vortex lattice calculations. The convenience lies in the fact that exact integrals of induced downwash can readily be obtained from which the accuracy of the corresponding vortex lattice values can be assessed. If the accuracy of the lattice for lifting-line calculations is established, it is reasonable to assume that the accuracy will also be satisfactory for lifting-plane theory, which is, after all, only an extension of lifting-line theory.

By a comparison of integrals as indicated above it has been proved that the standard loading functions when used with the lattice of 0·1 semispan spacing lead to accurate integrals of downwash. If, however, the P functions, which are much less regular than the standard functions, are used with the 0·1 lattice, greater inaccuracies than can be tolerated occur in the integrals of downwash. This difficulty could be overcome at the expense of considerable labour by decreasing the spacing of the lattice, but a simpler method, involving a minimum of work, is to retain the 0·1 spacing and vary the functions in such a manner that the integrals of downwash will be correct. The function will then have two sets of values, the first the true values to be used in analysing the properties of the wing subsequent to the establishment of the formula for the vortex sheet, and the second special values to be used with the lattice to obtain correct integrals of downwash.

The second set of values is found in the following way, the argument applying to the standard lattice of 0·1 semispan spacing. The lifting line is set out by the standard lattice as shown in Fig. 16, and the downwash factors obtained by the standard method demonstrated in Table 2. The relative distances are all zero, and the downwash factors follow the simple sequence 2·0000, $2\ (\frac{1}{3} - 1)$, $2\ [1/(2n + 1) - 1/(2n - 1)]$; etc., with a modification for the end corrector vortices. The downwash factors are shown in Table 44; if then, K_0 to K_{10} are regarded as the unknowns, the induced downwash can be expressed for points 0 to 8 as equations in the unknown quantities, as in Table 45. The constant column depends upon the distribution of downwash it is intended to represent, and the 0·1 spacing limits the argument to polygonal distributions with similar spacing. For example, the equations of Table 45 referring to the function P_a will have a constant column — 1 for point 0 and zero for the remaining points, while the column for P_b will be — 1 for point 0, — 0·5 for point 1, and zero for the remainder. After the application of a factor which occurs in the analysis, the two columns appear as in Table 45. In order to reduce the number of variables to 9 it is assumed that the values of K_9 and K_{10} coincide with the true values. Solution of the equations leads to the values defined by the term '0·1 lattice values' which are given for P_a and P_b in Table 46 against the true values, and are also plotted in Fig. 8.

It should be added that, the equations having been solved by elimination, it is an easy matter to compute the solution for any additional constant column by following the method described in section 7.1.

REFERENCES

No.	*Author*	*Title, etc.*
1	V. M. Falkner	The Calculation of Aerodynamic Loading on Surfaces of any Shape. R. & M. 1910.
2	V. M. Falkner	The Effect of Pointed Tips on Wing Loading Calculations. R. & M. 2483.
3	Whittaker and Robinson ..	*Calculus of Observations.* Blackie & Son.
4	The Staff of Mathematics Division N.P.L.	Tables of Complete Downwash due to a Rectangular Vortex. R. & M. 2461.
5	W. G. Bickley	Note on Falkner's Modification of Simpson's Rule. A.R.C. Report 9853.
6	H. Glauert	*The Elements of Aerofoil and Airscrew Theory.* Cambridge University Press.
7	V. M. Falkner	Tables of Multhopp and other Functions for use in Lifting Line and Lifting Plane Theory. Appendix by E. J. Watson. A.R.C. Report 11234. (To be published.)
8	E. W. Hobson	*Plane Trigonometry.* Second edition. Cambridge University Press.

Table I.

Numerical Values of Loading Functions.

	0	0·025	0·050	0·075	0·100	0·125	0·150	0·175	0·200	0·225	0·250
$\sqrt{1-\eta^2}$	1·0000	0·9997	0·9987	0·9972	0·9950	0·9922	0·9887	0·9846	0·9798	0·9744	0·9682
$\eta\sqrt{1-\eta^2}$	0	0·0250	0·0499	0·0748	0·0995	0·1240	0·1483	0·1723	0·1960	0·2192	0·2421
$\eta^2\sqrt{1-\eta^2}$	0	0·0006	0·0025	0·0056	0·0099	0·0155	0·0222	0·0302	0·0392	0·0493	0·0605
$\eta^3\sqrt{1-\eta^2}$	0	0	0·0001	0·0004	0·0010	0·0019	0·0033	0·0053	0·0078	0·0111	0·0151
$\eta^4\sqrt{1-\eta^2}$	0	0	0	0	0·0001	0·0002	0·0005	0·0009	0·0016	0·0025	0·0038
$\eta^5\sqrt{1-\eta^2}$	0	0	0	0	0	0	0·0001	0·0002	0·0003	0·0006	0·0009
$\eta^6\sqrt{1-\eta^2}$	0	0	0	0	0	0	0	0	0·0001	0·0001	0·0002
$\eta^7\sqrt{1-\eta^2}$	0	0	0	0	0	0	0	0	0	0	0·0001
$\eta^8\sqrt{1-\eta^2}$	0	0	0	0	0	0	0	0	0	0	0
$\eta^9\sqrt{1-\eta^2}$	0	0	0	0	0	0	0	0	0	0	0
$\eta^{10}\sqrt{1-\eta^2}$	0	0	0	0	0	0	0	0	0	0	0
	0·275	0·300	0·325	0·350	0·375	0·400	0·425	0·450	0·475	0·500	0·525
$\sqrt{1-\eta^2}$	0·9614	0·9539	0·9457	0·9367	0·9270	0·9165	0·9052	0·8930	0·8800	0·8660	0·8511
$\eta\sqrt{1-\eta^2}$	0·2644	0·2862	0·3074	0·3279	0·3476	0·3666	0·3847	0·4019	0·4180	0·4330	0·4468
$\eta^2\sqrt{1-\eta^2}$	0·0727	0·0859	0·0999	0·1148	0·1304	0·1466	0·1635	0·1808	0·1985	0·2165	0·2346
$\eta^3\sqrt{1-\eta^2}$	0·0200	0·0258	0·0325	0·0402	0·0489	0·0587	0·0695	0·0814	0·0943	0·1083	0·1232
$\eta^4\sqrt{1-\eta^2}$	0·0055	0·0077	0·0106	0·0141	0·0183	0·0235	0·0295	0·0366	0·0448	0·0541	0·0647
$\eta^5\sqrt{1-\eta^2}$	0·0015	0·0023	0·0034	0·0049	0·0069	0·0094	0·0126	0·0165	0·0213	0·0271	0·0339
$\eta^6\sqrt{1-\eta^2}$	0·0004	0·0007	0·0011	0·0017	0·0026	0·0038	0·0053	0·0074	0·0101	0·0135	0·0178
$\eta^7\sqrt{1-\eta^2}$	0·0001	0·0002	0·0004	0·0006	0·0010	0·0015	0·0023	0·0033	0·0048	0·0068	0·0094
$\eta^8\sqrt{1-\eta^2}$	0	0·0001	0·0001	0·0002	0·0004	0·0006	0·0010	0·0015	0·0023	0·0034	0·0049
$\eta^9\sqrt{1-\eta^2}$	0	0	0	0·0001	0·0001	0·0002	0·0004	0·0007	0·0011	0·0017	0·0026
$\eta^{10}\sqrt{1-\eta^2}$	0	0	0	0	0·0001	0·0001	0·0002	0·0003	0·0005	0·0008	0·0014
	0·550	0·575	0·600	0·625	0·650	0·675	0·700	0·725	0·750	0·775	0·800
$\sqrt{1-\eta^2}$	0·8352	0·8182	0·8000	0·7806	0·7599	0·7378	0·7141	0·6887	0·6614	0·6320	0·6000
$\eta\sqrt{1-\eta^2}$	0·4593	0·4704	0·4800	0·4879	0·4940	0·4980	0·4999	0·4993	0·4961	0·4898	0·4800
$\eta^2\sqrt{1-\eta^2}$	0·2526	0·2705	0·2880	0·3049	0·3211	0·3362	0·3499	0·3620	0·3721	0·3796	0·3840
$\eta^3\sqrt{1-\eta^2}$	0·1390	0·1555	0·1728	0·1906	0·2087	0·2269	0·2450	0·2625	0·2790	0·2942	0·3072
$\eta^4\sqrt{1-\eta^2}$	0·0764	0·0894	0·1037	0·1191	0·1357	0·1532	0·1715	0·1903	0·2093	0·2280	0·2458
$\eta^5\sqrt{1-\eta^2}$	0·0420	0·0514	0·0622	0·0744	0·0882	0·1034	0·1200	0·1380	0·1570	0·1767	0·1966
$\eta^6\sqrt{1-\eta^2}$	0·0231	0·0296	0·0373	0·0465	0·0573	0·0698	0·0840	0·1000	0·1177	0·1369	0·1573
$\eta^7\sqrt{1-\eta^2}$	0·0127	0·0170	0·0224	0·0291	0·0373	0·0471	0·0588	0·0725	0·0883	0·1061	0·1258
$\eta^8\sqrt{1-\eta^2}$	0·0070	0·0098	0·0134	0·0182	0·0242	0·0318	0·0412	0·0526	0·0662	0·0822	0·1007
$\eta^9\sqrt{1-\eta^2}$	0·0038	0·0056	0·0081	0·0114	0·0157	0·0215	0·0288	0·0381	0·0497	0·0637	0·0805
$\eta^{10}\sqrt{1-\eta^2}$	0·0021	0·0032	0·0048	0·0071	0·0102	0·0145	0·0202	0·0276	0·0372	0·0494	0·0644
	0·825	0·850	0·875	0·900	0·925	0·950	0·975	1·000	0·9625	0·98125	0·990625
$\sqrt{1-\eta^2}$	0·5651	0·5268	0·4841	0·4359	0·3800	0·3122	0·2222	0	0·2713	0·1927	0·1366
$\eta\sqrt{1-\eta^2}$	0·4662	0·4478	0·4236	0·3923	0·3515	0·2966	0·2166	0	0·2611	0·1891	0·1353
$\eta^2\sqrt{1-\eta^2}$	0·3846	0·3806	0·3707	0·3531	0·3251	0·2818	0·2112	0	0·2513	0·1856	0·1341
$\eta^3\sqrt{1-\eta^2}$	0·3173	0·3235	0·3243	0·3178	0·3007	0·2677	0·2060	0	0·2419	0·1821	0·1328
$\eta^4\sqrt{1-\eta^2}$	0·2618	0·2750	0·2838	0·2860	0·2782	0·2543	0·2008	0	0·2328	0·1787	0·1316
$\eta^5\sqrt{1-\eta^2}$	0·2160	0·2337	0·2483	0·2574	0·2573	0·2416	0·1958	0	0·2241	0·1753	0·1303
$\eta^6\sqrt{1-\eta^2}$	0·1782	0·1987	0·2173	0·2316	0·2380	0·2295	0·1909	0	0·2157	0·1720	0·1291
$\eta^7\sqrt{1-\eta^2}$	0·1470	0·1689	0·1901	0·2085	0·2202	0·2181	0·1861	0	0·2076	0·1688	0·1279
$\eta^8\sqrt{1-\eta^2}$	0·1213	0·1435	0·1663	0·1876	0·2036	0·2072	0·1815	0	0·1998	0·1657	0·1267
$\eta^9\sqrt{1-\eta^2}$	0·1001	0·1220	0·1456	0·1689	0·1884	0·1968	0·1769	0	0·1923	0·1625	0·1255
$\eta^{10}\sqrt{1-\eta^2}$	0·0825	0·1037	0·1274	0·1520	0·1742	0·1870	0·1725	0	0·1851	0·1595	0·1243

TABLE 2. FORMATION OF EQUATION FOR 21 VORTEX LATTICE.

		PORT										STARBOARD									
POSITION ON SPAN		0·9625	0·9	0·8	0·7	0·6	0·5	0·4	0·3	0·2	0·1	0	0·1	0·2	0·3	0·4	0·5	0·6	0·7	0·8	0·9	0·9625
DISTANCE BACK OF VORTEX		14·775	13·975	12·700	11·425	10·150	8·875	7·600	6·325	5·050	3·775	2·500	3·775	5·050	6·325	7·600	8·875	10·150	11·425	12·700	13·975	14·775
REL DISTANCES TO PT. 1. [0·2, 9·550]		5·223	4·425	3·150	1·875	0·600	-0·675	-1·950	-3·225	-4·500	-5·775	-7·050	-5·775	-4·500	-3·225	-1·950	-0·675	0·600	1·875	3·150	4·425	5·223
LOAD FUNCTION $\sqrt{1-\eta^2}$		0·2713	0·4359	0·6000	0·7141	0·8000	0·8660	0·9165	0·9539	0·9798	0·9950	1·0000	0·9950	0·9798	0·9539	0·9165	0·8660	0·8000	0·7141	0·6000	0·4359	0·2713
DOWNWASH FACTORS	E	-0·001	-0·003	-0·004	-0·006	-0·008	-0·011	-0·016	-0·026	-0·047	-0·097	-0·250	-1·306	4·049	-1·258	-0·195	-0·064	-0·029	-0·016	-0·010	-0·007	-0·001

$$\omega/V = 20 \sum E\sqrt{1-\eta^2}\, a_0 = 20\, a_0 \quad [0.73342] = 14·6684\, a_0 \text{ PER RADIAN INCIDENCE.}$$

TABLE 3 FORMATION OF EQUATION FOR 126 VORTEX LATTICE.

		POSITION ON SPAN	0·9625	0·9	0·8	0·7	0·6	0·5	0·4	0·3	0·2	0·1	0	0·1	0·2	0·3	0·4	0·5	0·6	0·7	0·8	0·9	0·9625
	40a + 3·5b										3·550	2·192	0·835	2·192	3·550	4·908	6·267	7·625	8·985				
	40a + 10 b										5·050	3·775	2·500	3·775	5·050	6·325	7·600	8·875	10·150				
	40a + 16·6 b	EXTEND AS REQUIRED.									6·550	5·358	4·167	5·358	6·550	7·742	8·933	10·125	11·317	EXTEND AS REQUIRED.			
VORTICES	40a + 25·3b										8·050	6·942	5·833	6·942	8·050	9·158	10·267	11·375	12·483				
	40a + 30 b										9·550	8·525	7·500	8·525	9·550	10·575	11·600	12·625	13·650				
	40a + 36·6b										11·050	10·108	9·167	10·108	11·050	11·992	12·933	13·875	14·817				
BACK OF	40a + 10 b		14·775	13·975	12·700	11·425	10·150	8·875	7·600	6·325	5·050	3·775						8·876	10·150	11·426	12·700	13·975	14·775
	40a + 20 b		16·070	15·350	14·200	13·050	11·900	10·750	9·600	8·450	7·300	6·150						10·750	11·900	13·050	14·200	15·350	16·070
DISTANCE	40a + 30 b		17·367	16·725	15·700	14·675	13·650	12·625	11·600	10·575	9·550	8·525						12·625	13·650	14·675	15·700	16·725	17·367
			4·473	3·675	2·400	1·125	-0·150	-1·425	-2·700	-3·975	-5·250	-6·525	-7·800	-6·525	-5·250	-3·975	-2·700	-1·425	-0·150	1·125	2·400	3·675	4·473
	POINT 2. RELATIVE DISTANCES [0·2, 10·300]		5·770	5·050	3·900	2·750	1·600	0·450	-0·700	-1·850	-3·000	-4·150	-5·300	-4·150	-3·000	-1·850	-0·700	0·450	1·600	2·750	3·900	5·050	5·770
			7·067	6·425	5·400	4·375	3·350	2·325	1·300	0·275	-0·750	-1·775	-2·800	-1·775	-0·750	0·275	1·300	2·325	3·350	4·375	5·400	6·425	7·067
											-2·250	-3·358	-4·467	-3·358	-2·250	-1·142	-0·033	1·075	2·183				
											-0·750	-1·775	-2·800	-1·775	-0·750	0·275	1·300	2·325	3·350				
											0·750	-0·192	-1·133	-0·192	0·750	1·692	2·633	3·575	4·517				
			4·473	3·675	2·400	1·126	-0·150	-1·425	-2·700	-3·975	-5·250	-6·525	-9·467	-8·108	-6·750	-5·392	-4·033	-1·425	-0·150	1·125	2·400	3·675	4·473
	POINT 2 RELATIVE DISTANCES [0·2, 10·300]		5·770	5·050	3·900	2·750	1·600	0·450	-0·700	-1·850	-3·000	-4·150	-7·800	-6·525	-5·250	-3·975	-2·700	0·450	1·600	2·750	3·900	5·050	5·770
							3·350	2·325	1·300	0·275	-0·750	-1·775	-6·133	-4·942	-3·750	-2·558	-1·367	2·325	3·350	4·375	5·400	6·425	7·067
													-4·467	-3·358	-2·250	-1·142	-0·033						
													-2·800	-1·775	-0·750	0·275	1·300						
													-1·133	-0·192	0·750	1·692	2·633						

LOAD FUNCTION $\sqrt{1-\eta^2}$		0·2713	0·4359	0·6000	0·7141	0·8000	0·8660	0·9165	0·9539	0·9798	0·9950	1·0000	0·9950	0·9798	0·9539	0·9165	0·8660	0·8000	0·7141	0·6000	0·4359	0·2713
POINT 2 DOWNWASH FACTORS 126/90	E1	-0·001	-0·003	-0·004	-0·006	-0·008	-0·011	-0·017	-0·028	-0·052	-0·103	-0·257	-1·319	4·022	-1·302	-0·230	-0·081	-0·037	-0·018	-0·011	-0·008	-0·002
	E2	-0·001	-0·003	-0·004	-0·005	-0·007	-0·010	-0·015	-0·024	-0·049	-0·100	-0·253	-1·312	4·036	-1·280	-0·211	-0·071	-0·032	-0·015	-0·010	-0·007	-0·001
	E3	-0·001	-0·003	-0·004	-0·005	-0·006	-0·009	-0·013	-0·020	-0·045	-0·094	-0·246	-1·297	4·070	-1·227	-0·174	-0·059	-0·028	-0·012	-0·008	-0·006	-0·001
	E4									-0·040	-0·086	-0·235	-1·263	4·189	-1·059	-0·134	-0·047	-0·023				
	E5									-0·035	-0·074	-0·212	-1·160	5·333	-0·547	-0·090	-0·036	-0·019				
	E6									-0·029	-0·059	-0·172	-0·751	-1·333	-0·184	-0·057	-0·027	-0·016				
SUM		-0·002	-0·006	-0·008	-0·011	-0·015	-0·021	-0·032	-0·052	-0·250	-0·516	-1·375	-7·102	20·317	-5·599	-0·901	-0·321	-0·155	-0·033	-0·021	-0·015	-0·003
POINT 2 DOWNWASH FACTORS 126/86	E1	-0·001	-0·003	-0·004	-0·006	-0·008	-0·011	-0·017	-0·028	-0·052	-0·103	-0·257	-1·319	4·022	-1·302	-0·230	-0·081	-0·037	-0·018	-0·011	-0·008	-0·002
	E2	-0·001	-0·003	-0·004	-0·005	-0·007	-0·010	-0·015	-0·024	-0·049	-0·100	-0·253	-1·312	4·036	-1·280	-0·211	-0·071	-0·032	-0·015	-0·010	-0·007	-0·001
	E3					-0·006	-0·009	-0·013	-0·020	-0·045	-0·094	-0·246	-1·297	4·070	-1·227	-0·179	-0·059	-0·028	-0·012	-0·008	-0·006	-0·001
	E4									-0·040	-0·086	-0·235	-1·263	4·189	-1·059	-0·134	-0·047	-0·023				
	E5									-0·035	-0·074	-0·212	-1·160	5·333	-0·547	-0·090	-0·036	-0·019				
	E6									-0·029	-0·059	-0·172	-0·751	-1·333	-0·184	-0·057	-0·027	-0·016				
SUM		-0·002	-0·006	-0·008	-0·011	-0·015	-0·021	-0·032	-0·052	-0·250	-0·516	-1·375	-7·102	20·317	-5·599	-0·901	-0·321	-0·155	-0·033	-0·021	-0·016	-0·003
POINT 2 DOWNWASH FACTORS 126/74	E1	-0·001	-0·003	-0·004	-0·006	-0·008	-0·011	-0·017	-0·028	-0·049	-0·100	-0·257	-1·319	4·022	-1·302	-0·230	-0·071	-0·032	-0·018	-0·011	-0·008	-0·002
	E2	-0·001	-0·003	-0·004	-0·005	-0·007	-0·010	-0·015	-0·024	-0·043	-0·090	-0·253	-1·312	4·036	-1·280	-0·211	-0·053	-0·025	-0·015	-0·010	-0·007	-0·001
	E3					-0·006	-0·009	-0·013	-0·020	-0·035	-0·074	-0·246	-1·297	4·070	-1·227	-0·179	-0·036	-0·019	-0·012	-0·008	-0·006	-0·001
	E4											-0·235	-1·263	4·189	-1·059	-0·134						
	E5											-0·212	-1·160	5·333	-0·547	-0·090						
	E6											-0·172	-0·751	-1·333	-0·184	-0·057						
SUM		-0·002	-0·006	-0·008	-0·011	-0·015	-0·021	-0·032	-0·052	-0·092	-0·190	-1·375	-7·102	20·317	-5·599	-0·901	-0·124	-0·067	-0·033	-0·021	-0·015	-0·003

INTEGRALS $\sum E\sqrt{1-\eta^2}$	
$\sum E_1\sqrt{1-\eta^2}$	0·66540
$\sum E_2\sqrt{1-\eta^2}$	0·74706
$\sum E_3\sqrt{1-\eta^2}$	0·90567
$\sum E_4\sqrt{1-\eta^2}$	1·29584
$\sum E_5\sqrt{1-\eta^2}$	3·10051
$\sum E_6\sqrt{1-\eta^2}$	-2·57638
$\sum E_1\sqrt{1-\eta^2}$	-0·08996
$\sum E_2\sqrt{1-\eta^2}$	-0·07848
$\sum (E_1-E_3)\sqrt{1-\eta^2}$	-0·02257
$\sum (1-6)$	4·13810
$\sum (7-8)$	-0·16844
ω/V PER RADIAN	
40 × 0·36011	a_0
40 × 0·21836	a_1
40 × 0·03113	a_2

126/90

INTEGRALS $\sum E\sqrt{1-\eta^2}$	
$\sum E_1\sqrt{1-\eta^2}$	0·66540
$\sum E_2\sqrt{1-\eta^2}$	0·74706
$\sum E_3\sqrt{1-\eta^2}$	0·90567
$\sum E_4\sqrt{1-\eta^2}$	1·29584
$\sum E_5\sqrt{1-\eta^2}$	3·10051
$\sum E_6\sqrt{1-\eta^2}$	-2·57638
$\sum E_1\sqrt{1-\eta^2}$	-0·08996
$\sum E_2\sqrt{1-\eta^2}$	-0·07848
$\sum (E_1-E_3)\sqrt{1-\eta^2}$	-0·02186
$\sum (1-6)$	4·13810
$\sum (7-8)$	-0·16844
ω/V PER RADIAN	
40 × 0·36011	a_0
40 × 0·21836	a_1
40 × 0·03122	a_2

126/86

INTEGRALS $\sum E\sqrt{1-\eta^2}$	
$\sum E_1\sqrt{1-\eta^2}$	0·91858
$\sum E_2\sqrt{1-\eta^2}$	0·98166
$\sum E_3\sqrt{1-\eta^2}$	1·11678
$\sum E_4\sqrt{1-\eta^2}$	1·47971
$\sum E_5\sqrt{1-\eta^2}$	3·25481
$\sum E_6\sqrt{1-\eta^2}$	-2·45308
$\sum E_1\sqrt{1-\eta^2}$	-0·32456
$\sum E_2\sqrt{1-\eta^2}$	-0·27606
$\sum (E_1-E_3)\sqrt{1-\eta^2}$	-0·10215
$\sum (1-6)$	5·29846
$\sum (7-8)$	-0·60062
ω/V PER RADIAN	
40 × 0·36520	a_0
40 × 0·21755	a_1
40 × 0·03124	a_2

126/74

Table 4

Chordwise location of pivotal points

Lattice	Terms included			Position of pivotal points
	cot θ/2	sin θ	sin 2θ	
21 vortex	*			¾ chord
84 vortex	*			¾ chord
	*	*		½, ¾ chord
	*	*	*	¼, ½, ¾ chord
126 vortex	*			⅚ chord
	*	*		⅜, ⅚ chord
	*	*	*	⅜, ⅝, ⅚ chord
328 vortex	*			¾ chord
	*	*		½, ¾ chord
	*	*	*	¼, ½, ¾ chord

Table 5

Table of integrals $\int_0^1 \eta^n \sqrt{1-\eta^2}\, d\eta$ and $\int_{-1}^1 \eta^n \sqrt{1-\eta^2}\, d\eta$

n	Integral $\int_0^1$	Integral $\int_{-1}^1$
0	$\pi/4$	$\pi/2$
1	1/3	0
2	$\pi/16$	$\pi/8$
3	2/15	0
4	$\pi/32$	$\pi/16$
5	8/105	0
6	$5\pi/256$	$5\pi/128$
7	16/315	0
8	$7\pi/512$	$7\pi/256$
9	128/3465	0
10	$21\pi/2048$	$21\pi/1024$
11	256/9009	0

Table 6

Table of distances for wing of Fig. 1

η	(a) Datum to L.E.	(b) Chord
0	0	0·2500
0·05	0·0175	0·2438
0·10	0·0350	0·2375
0·15	0·0525	0·2312
0·20	0·0700	0·2250
0·25	0·0875	0·2188
0·30	0·1050	0·2125
0·35	0·1225	0·2062
0·40	0·1400	0·2000
0·45	0·1575	0·1938
0·50	0·1750	0·1875
0·55	0·1925	0·1812
0·60	0·2100	0·1750
0·65	0·2275	0·1688
0·70	0·2450	0·1625
0·75	0·2625	0·1562
0·80	0·2800	0·1500
0·85	0·2975	0·1438
0·90	0·3150	0·1376
0·95	0·3325	0·1312
0·9625	0·3369	0·1297
1·000	0·3500	0·1250

Table 7

Factors to represent chordwise functions as line vortices

Solution	Position on chord from L.E.	$\cot \theta/2$	$\sin \theta$	$\sin 2\theta$
1 or 2 point	0·25	0·5	0	0·125
	0·50	0	0·25	0
	0·75	0	0	−0·125
4 point	0·125	0·2734	0·0488	0·0732
	0·375	0·1172	0·0762	0·0381
	0·625	0·0703	0·0762	−0·0381
	0·875	0·0391	0·0488	−0·0732
6 point	0·0833	0·2256	0·0273	0·0456
	0·2500	0·1025	0·0456	0·0455
	0·4167	0·0684	0·0521	0·0174
	0·5833	0·0488	0·0521	−0·0174
	0·7500	0·0342	0·0456	−0·0455
	0·9167	0·0205	0·0273	−0·0456
8 point	0·0625	0·1964	0·0180	0·0315
	0·1875	0·0916	0·0308	0·0385
	0·3125	0·0635	0·0368	0·0276
	0·4375	0·0480	0·0394	0·0099
	0·5625	0·0374	0·0394	−0·0099
	0·6875	0·0289	0·0368	−0·0276
	0·8125	0·0211	0·0308	−0·0385
	0·9375	0·0131	0·0180	−0·0315

Table 8

Example of normalisation and solution

Before normalisation

	x_1	x_2	x_3	x_4		Sum
1	1·854	−2·560	3·220	−1·000		1·514
2	1·642	−2·105	1·504	−1·200	= 0	−0·159
3	1·518	−1·498	0·292	−1·400		−1·088
4	1·307	−0·860	−0·499	−1·600		−1·652
5	1·119	−0·115	−1·536	−1·800		−2·332

Normalisation and solution

	x_1	x_2	x_3	x_4	Sum	Check	Factors
6	11·398	−11·729	6·512	−10·055	−3·874	−3·874	0·42495
7	−11·729	15·981	−11·241	8·766	−0·223	−0·222	0·73556
8	6·512	−11·241	16·324	−1·870	8·725	8·725	*
9	8·631	−6·962	0·080	−9·260	−7·581	−7·582	*
10	−6·952	5·736	0·000	7·394	6·177	6·177	0·8249
11	0·168	0·000	0·000	−0·245	−0·077	−0·077	

	Roots
x_1	1·458
x_2	0·478
x_3	−0·147
x_4	1·000

Row	Residuals
1	0·006
2	−0·033
3	0·054
4	−0·032
5	0·002
6	0·000
7	0·000
8	−0·001

Solution with additional constant column

x_4 before normalisation	x_4 after normalisation	Factors	x_4	Factors	x_4
−1·200	−10·236	0·42495	−8·952	*	−0·222
−1·300	9·380	0·73556	7·163	0·8249	
−1·400	−3·022	*			
−1·500					
−1·600					

	Roots
x_1	1·321
x_2	0·352
x_3	−0·106
x_4	1·000

Table 9 Equations for 6 point solution for a delta wing

Solution 3 Incidence

Point	a_0	a_1	c_0	c_1	e_0	e_1	1		Sum
1	0·23801	0·06849	-0·01590	-0·00405	-0·00972	-0·00329	-0·02500		0·24854
2	0·20883	0·11411	-0·04039	-0·01619	-0·01866	-0·00804	-0·02500		0·21466
3	0·28320	0·01214	0·32032	0·06821	0·24082	0·05951	-0·02500		0·95920
4	0·27181	0·15761	0·29745	0·16036	0·20951	0·11328	-0·02500	= 0	1·18502
5	0·24211	0·03580	0·15343	0·04476	0·04852	0·01599	-0·02500		0·51561
6	0·23268	0·13117	0·12927	0·07082	0·02352	0·01620	-0·02500		0·57866

Solution 17 Linear wing twist

Point	a_1	c_0	c_1	e_0	e_1	α_0	1		Sum
1	-0·05051	-0·07540	-0·03380	-0·03947	-0·01816	-0·02500	-0·00500		-0·24734
2	0·00969	-0·09260	-0·04230	-0·04476	-0·02110	-0·02500	-0·00500		-0·22107
3	-0·12946	0·24952	0·03281	0·20542	0·04181	-0·02500	-0·02000		0·35510
4	0·02170	0·22950	0·12639	0·17553	0·09629	-0·02500	-0·02000	= 0	0·60441
5	-0·08526	0·09290	0·01450	0·01826	0·00085	-0·02500	-0·01500		0·00125
6	0·01483	0·07110	0·04174	-0·00557	0·00166	-0·02500	-0·01500		0·08376

Table 10

Table of distances for delta wing

η	a Datum to leading edge	b Chord
0	0	0·8660
0·05	0·0433	0·8227
0·10	0·0866	0·7794
0·15	0·1299	0·7361
0·20	0·1732	0·6928
0·25	0·2165	0·6495
0·30	0·2598	0·6062
0·35	0·3031	0·5629
0·40	0·3464	0·5196
0·45	0·3897	0·4763
0·50	0·4330	0·4330
0·55	0·4763	0·3897
0·60	0·5196	0·3464
0·65	0·5629	0·3031
0·70	0·6062	0·2598
0·75	0·6495	0·2165
0·80	0·6928	0·1732
0·85	0·7361	0·1299
0·90	0·7794	0·0866
0·95	0·8227	0·0433
1·00	0·8660	0

Table 11 Calculation of wing properties for delta wing, solution 3

(1)	(2)	(3)	(4)	(5)	(6)	(7)	(8)	(9)	(10)
η	$F_0+\frac{1}{2}F_1$	$F_0+F_1-\frac{1}{2}F_2$	$\frac{0.25(3)}{(2)}$	$a+b(4)$	(2) × (5)	Factors	$K/4sV$	$C/2s$	C_{LL} for $C_L=1$
0	0.1157	0.1403	0.303	0.262	0.0304	1	0.364	0.8660	0.670
0.05	0.1155	0.1398	0.303	0.292	0.0338	4	0.363	0.8227	0.701
0.10	0.1150	0.1386	0.301	0.321	0.0370	2	0.361	0.7794	0.736
0.15	0.1141	0.1365	0.299	0.350	0.0399	4	0.358	0.7361	0.773
0.20	0.1128	0.1336	0.296	0.378	0.0427	2	0.354	0.6928	0.812
0.25	0.1110	0.1300	0.293	0.407	0.0452	4	0.349	0.6495	0.853
0.30	0.1090	0.1257	0.288	0.435	0.0474	2	0.342	0.6062	0.897
0.35	0.1064	0.1209	0.284	0.463	0.0493	4	0.334	0.5629	0.944
0.40	0.1035	0.1155	0.279	0.491	0.0509	2	0.325	0.5196	0.994
0.45	0.1001	0.1096	0.274	0.520	0.0521	4	0.314	0.4763	1.049
0.50	0.0962	0.1034	0.269	0.549	0.0529	2	0.302	0.4330	1.109
0.55	0.0919	0.0970	0.264	0.579	0.0532	4	0.289	0.3897	1.176
0.60	0.0869	0.0903	0.260	0.610	0.0530	2	0.273	0.3464	1.252
0.65	0.0814	0.0835	0.256	0.641	0.0522	4	0.256	0.3031	1.341
0.70	0.0753	0.0766	0.254	0.672	0.0506	2	0.237	0.2598	1.447
0.75	0.0685	0.0695	0.254	0.704	0.0482	4	0.215	0.2165	1.579
0.80	0.0608	0.0621	0.255	0.737	0.0448	2	0.191	0.1732	1.752
0.85	0.0521	0.0541	0.260	0.770	0.0401	4	0.164	0.1299	2.002
0.90	0.0419	0.0448	0.267	0.803	0.0336	1.800	0.132	0.0866	2.415
0.95	0.0290	0.0325	0.280	0.835	0.0243	4.525	0.091	0.0433	3.348
1.00	0	0	0.298	0.866	0.0000	0.675	0	0	

a.c = 2.6154/5.2058 = 0.5024 Span = 1.160 $\bar{c}$ behind apex $\bar{c}$ = 0.4330 Span

Table 12 Calculation of wing properties for solution 17

(1)	(2)	(3)	(4)	(5)	(6)	(7)	(8)
η	$F_0+\frac{1}{2}F_1$	$F_0+F_1-\frac{1}{2}F_2$	$\frac{0.25(3)}{(2)}$	$a+b(4)$	(2) × (5)	Factors	$K/4sV$ per rad.
0	−0.01307	−0.00466	0.0891	0.0772	−0.00101	1	−0.0411
0.05	−0.01288	−0.00452	0.0877	0.1154	−0.00149	4	−0.0405
0.10	−0.01233	−0.00411	0.0833	0.1515	−0.00187	2	−0.0387
0.15	−0.01142	−0.00343	0.0751	0.1852	−0.00212	4	−0.0359
0.20	−0.01018	−0.00251	0.0616	0.2159	−0.00220	2	−0.0320
0.25	−0.00864	−0.00137	0.0396	0.2422	−0.00209	4	−0.0271
0.30	−0.00684	−0.00004	0.0015	0.2607	−0.00178	2	−0.0215
0.35	−0.00484	0.00142	−0.0733	0.2618	−0.00127	4	−0.0152
0.40	−0.00271	0.00298	−0.2749	0.2036	−0.00055	2	−0.0085
0.45	−0.00048	0.00459	−2.3906	−0.7489	0.00036	4	−0.0015
0.50	0.00175	0.00618	0.8829	0.8153	0.00143	2	0.0055
0.55	0.00390	0.00768	0.4923	0.6682	0.00261	4	0.0123
0.60	0.00590	0.00905	0.3835	0.6524	0.00385	2	0.0185
0.65	0.00766	0.01019	0.3326	0.6637	0.00508	4	0.0241
0.70	0.00907	0.01104	0.3043	0.6853	0.00622	2	0.0285
0.75	0.01006	0.01151	0.2860	0.7114	0.00716	4	0.0316
0.80	0.01050	0.01150	0.2738	0.7402	0.00777	2	0.0330
0.85	0.01028	0.01092	0.2656	0.7706	0.00792	4	0.0323
0.90	0.00923	0.00959	0.2598	0.8019	0.00740	1.800	0.0290
0.95	0.00699	0.00716	0.2561	0.8338	0.00583	4.525	0.0220
1.00	0	0	0.2537	0.8660	0.00000	0.675	0

$$C_{m_0} = -\frac{64\,\pi s^4}{S\bar{c}^2}\int_0^1 (\text{col } 6)\,d\eta = -67.021\ \frac{0.12908}{60} = -0.1442$$

Table 13

Additional equations for incidence solution

Point	a_0	a_1	c_0	c_1	e_0	e_1	1	Residuals solution 5
7	0·31090	0·12395	-0·03386	-0·01042	-0·00484	-0·00185	-0·02500	0·00901
8	0·21707	0·12335	-0·06015	-0·02601	-0·01191	-0·00511	-0·02500	0·00137
9	0·25473	0·08309	-0·05115	-0·00951	-0·00680	-0·00249	-0·02500	0·00199
10	0·20953	0·11497	-0·05562	-0·02394	-0·01387	-0·00602	-0·02500	0·00027

Table 14

Additional equations for linear twist solution

Point	a_1	c_0	c_1	e_0	e_1	α_0	1	Residuals solution 17
7	-0·03150	-0·11158	-0·04928	-0·04370	-0·02128	0·02500	0	0·00289
8	0·01482	-0·11442	-0·05314	-0·03904	-0·01867	0·02500	0	0·00340
9	-0·04428	-0·09484	-0·04135	-0·03864	-0·01842	-0·02500	-0·00250	0·00117
10	0·01020	-0·10800	-0·05013	-0·04006	-0·01912	-0·02500	-0·00250	0·00130

Table 15

Equations for establishing P functions Incidence

Point	a_0'	a_1'	P_{a0}	P_{a1}	P_{b0}	P_{b1}	1	
1	0·23801	0·06849	0·00481	0·00003	0·01014	0·00033	0	
2	0·20885	0·11411	0·00306	0·00244	0·00644	0·00307	0	
7	0·31090	0·12395	0·13751	0·04548	0·15139	0·05247	0·00901	= 0
8	0·21707	0·12334	0·15504	0·07379	0·15939	0·07766	0·00137	
9	0·25473	0·08309	0·00675	0·00144	0·07692	0·02349	0·00199	
10	0·20953	0·11497	0·00343	0·00280	0·08242	0·04079	0·00027	

Table 16

Equations for establishing P functions Linear wing twist

Point	a_1'	P_{a0}	P_{a1}	P_{b0}	P_{b1}	α_0	1	
1	-0·05052	-0·14659	-0·07567	-0·02006*	-0·01477	-0·02500	0	
2	0·00970	-0·12978	-0·06398	-0·02006*	-0·00818	-0·02500	0	
7	-0·03150	-0·06025	-0·05340	0·11194	0·03274	-0·02500	0·00289	= 0
8	0·01482	0·01696	0·00476	0·13184	0·06389	-0·02500	0·00340	
9	-0·04428	-0·15528	-0·07958	0·04469	0·00733	-0·02500	0·00117	
10	0·01020	-0·12985	-0·06384	0·05583	0·02750	-0·02500	0·00130	

* The agreement is fortuitous

Table 17

Solution 7

Point	a_0'	p_{a0}	p_{b0}	1	
1	0·10103	0·00475	0·00947	0	= 0
2	-0·01939	-0·00182	-0·00371	0	
7	0·06300	0·04655	0·04645	0·00901	
8	-0·02963	0·00746	0·00406	0·00137	
9	0·08855	0·00387	0·02995	0·00199	
10	-0·02041	-0·00217	0·00083	0·00027	

Table 18

Solution 8

Point	a_0'	p_0	1	
1	0·10103	0·00640	0	= 0
2	-0·01939	-0·00248	0	
7	0·06300	0·04652	0·00901	
8	-0·02963	0·00627	0·00137	

Table 19

Point	a_1'	p_0	p_1	α_0	1	
1	-0·05062	-0·04537	-0·02695	-0·02500	0	= 0
2	0·00970	-0·04200	-0·01934	-0·02500	0	
7	-0·03150	0·07750	0·01551	-0·02500	0·00289	
8	0·01482	0·10886	0·05206	-0·02500	0·00340	
9	-0·04428	0·00462	0·01005	-0·02500	0·00117	
10	0·01020	0·01869	0·00923	-0·02500	0·00130	

Table 20 Solution 1 21 vortex incidence

a_0 0·11016 $dc_L/d\alpha = 2·402$ $C_{Di} = 0·1392\, c_L^2$
c_0 -0·01006
e_0 -0·01824
a.c. 1·116 $\bar{c}$ behind apex
Local a.c. 0·25 chord

η	K/4s V per rad.	C_{LL}	η	K/4s V per rad.	C_{LL}
0	0·346	0·666	0·60	0·262	1·259
0·10	0·344	0·735	0·70	0·226	1·450
0·20	0·338	0·812	0·80	0·181	1·745
0·30	0·327	0·898	0·90	0·123	2·372
0·40	0·311	0·998	0·95	0·085	3·253
0·50	0·290	1·114	1·00	0	

Table 21 Solution 2 21 vortex incidence

a_0 0·11029 $dc_L/d\alpha$ 2·408
c_0 -0·00836 Local a.c. 0·25 chord
e_0 -0·02035 C_{Di} 0·1392 c_L^2

Table 22 Solution 3 126 vortex incidence

a_0 0·09117 c_0 0·06813 e_0 -0·08670
a_1 0·04912 c_1 -0·16805 e_1 0·15296

$dc_L/d\alpha = 2·518$ a.c. 1·160 $\bar{c}$ behind apex
$C_{Di} = 0·1390\, c_L^2$

η	K/4s V per rad.	C_{LL}	Local a.c.	η	K/4s V per rad.	C_{LL}	Local a.c.
0	0·364	0·667	0·303	0·55	0·289	1·176	0·264
0·05	0·363	0·701	0·303	0·60	0·273	1·252	0·260
0·10	0·361	0·736	0·301	0·65	0·256	1·341	0·256
0·15	0·358	0·773	0·299	0·70	0·237	1·447	0·254
0·20	0·354	0·812	0·296	0·75	0·215	1·579	0·254
0·25	0·349	0·853	0·293	0·80	0·191	1·752	0·256
0·30	0·342	0·897	0·288	0·85	0·164	2·002	0·260
0·35	0·334	0·944	0·284	0·90	0·132	2·415	0·267
0·40	0·325	0·994	0·279	0·95	0·091	3·348	0·280
0·45	0·314	1·049	0·274	1·00	0		0·298
0·50	0·302	1·109	0·269				

Table 23 Solution 4 126 Vortex incidence

a_0 0·07610 c_0 0·12971 e_0 −0·13419

a_1 0·07688 c_1 −0·28304 e_1 0·24520

a_2 0·01972 c_2 −0·07759 e_2 0·05529

$dc_L/d\alpha$ = 2·499 a.c. 1·168 $\bar{c}$ behind apex

$c_{Di} = 0·1388\ c_L^2$

η	K/4sV per rad.	C_{LL}	Local a.c.	η	K/4sV per rad.	C_{LL}	Local a.c.
0	0·358	0·662	0·312	0·55	0·287	1·179	0·263
0·05	0·358	0·696	0·311	0·60	0·272	1·258	0·258
0·10	0·356	0·731	0·309	0·65	0·255	1·349	0·254
0·15	0·353	0·768	0·307	0·70	0·237	1·458	0·251
0·20	0·350	0·808	0·303	0·75	0·216	1·593	0·251
0·25	0·344	0·849	0·299	0·80	0·192	1·772	0·263
0·30	0·338	0·893	0·293	0·86	0·165	2·028	0·259
0·35	0·331	0·941	0·288	0·90	0·133	2·452	0·268
0·40	0·322	0·992	0·282	0·95	0·092	3·406	0·284
0·45	0·312	1·048	0·275	1·00	0		0·306
0·50	0·300	1·110	0·269				

Table 24 Solution 5 328 Vortex incidence

a_0 0·08092 c_0 0·11414 e_0 −0·12499

a_1 0·08016 c_1 −0·28145 e_1 0·25000

a_2 0·02236 c_2 −0·06446 e_2 0·04038

$dc_L/d\alpha$ = 2·606 a.c. 1·162 $\bar{c}$ behind apex

$c_{Di} = 0·1392\ c_L^2$

η	K/4sV per rad.	C_{LL}	Local a.c.	η	K/4sV per rad.	C_{LL}	Local a.c.
0	0·380	0·674	0·310	0·55	0·296	1·167	0·263
0·05	0·379	0·708	0·309	0·60	0·280	1·241	0·258
0·10	0·377	0·743	0·308	0·65	0·262	1·327	0·254
0·15	0·374	0·780	0·305	0·70	0·242	1·431	0·252
0·20	0·369	0·818	0·302	0·75	0·220	1·562	0·252
0·25	0·363	0·858	0·297	0·80	0·196	1·737	0·256
0·30	0·355	0·900	0·286	0·85	0·168	1·990	0·263
0·35	0·346	0·945	0·280	0·90	0·136	2·414	0·275
0·40	0·336	0·993	0·274	0·95	0·095	3·372	0·292
0·45	0·324	1·045	0·268	1·00	0		0·317
0·50	0·311	1·103					

Table 25 Solution 6 328 Vortex incidence

a_0 0·08324 c_0 0·09380 e_0 −0·09955

a_1 0·07640 c_1 −0·24144 e_1 0·19907

a_2 0·01785 c_2 −0·03353 e_2 0·00486

$dc_L/d\alpha$ = 2·614 a.c. 1·163 $\bar{c}$ behind apex.

$c_{Di} = 0·1392\ c_L^2$

η	K/4sV per rad.	C_{LL}	Local a.c.	η	K/4sV per rad.	C_{LL}	Local a.c.
0	0·382	0·674	0·310	0·55	0·297	1·167	0·265
0·05	0·381	0·708	0·310	0·60	0·281	1·240	0·260
0·10	0·379	0·744	0·308	0·65	0·263	1·326	0·256
0·15	0·375	0·780	0·306	0·70	0·243	1·430	0·254
0·20	0·370	0·818	0·302	0·75	0·221	1·561	0·254
0·25	0·364	0·858	0·298	0·80	0·196	1·736	0·256
0·30	0·357	0·900	0·294	0·85	0·169	1·988	0·262
0·35	0·348	0·945	0·288	0·90	0·136	2·410	0·272
0·40	0·337	0·993	0·282	0·95	0·095	3·366	0·287
0·45	0·325	1·045	0·276	1·00	0		0·309
0·50	0·312	1·103	0·270				

Table 26 Solution 7 126 Vortex incidence

a_0' 0·01365 $dc_L/d\alpha$ = 2·518

p_{a0} −0·12092 $c_{Di} = 0·1390\ c_L^2$

p_{b0} −0·08995

η	K/4sV per rad	C_{LL}	Local a.c.	η	K/4sV per rad.	C_{LL}	Local a.c.
0	0·364	0·667	0·358	0·55	0·289	1·170	0·264
0·05	0·363	0·701	0·351	0·60	0·273	1·252	0·260
0·10	0·361	0·736	0·339	0·65	0·256	1·341	0·256
0·15	0·358	0·773	0·327	0·70	0·237	1·447	0·254
0·20	0·354	0·812	0·317	0·75	0·215	1·579	0·254
0·25	0·349	0·853	0·309	0·80	0·191	1·752	0·255
0·30	0·342	0·897	0·300	0·85	0·164	2·002	0·260
0·35	0·334	0·944	0·293	0·90	0·132	2·415	0·267
0·40	0·325	0·994	0·286	0·95	0·091	3·348	0·280
0·45	0·314	0·049	0·278	1·00	0		0·298
0·50	0·302	0·109	0·271				

Table 27 Solution 8 126 vortex incidence

a_0' 0·01247
a_1' -0·02494
p_0 -0·20912
p_1 0·41824

$dC_L/d\alpha$ = 2·518
C_{Di} = 0·1390 C_L^2
a.c. 1·183 $\bar{c}$ behind apex

η	K/4sV per rad	C_{LL}	Local a.c.	η	K/4sV per rad	C_{LL}	Local a.c.
0	0·364	0·667	0·356	0·55	0·289	1·176	0·264
0·05	0·363	0·701	0·349	0·60	0·273	1·252	0·260
0·10	0·361	0·736	0·337	0·65	0·256	1·341	0·256
0·15	0·358	0·773	0·326	0·70	0·237	1·447	0·254
0·20	0·354	0·812	0·316	0·75	0·215	1·579	0·254
0·25	0·349	0·853	0·308	0·80	0·191	1·752	0·255
0·30	0·342	0·897	0·300	0·85	0·164	2·002	0·260
0·35	0·334	0·944	0·293	0·90	0·132	2·415	0·267
0·40	0·325	0·994	0·286	0·95	0·091	3·348	0·280
0·45	0·314	1·049	0·278	1·00	0		0·298
0·50	0·302	1·109	0·272				

Table 28 Solution 9 21 vortex incidence

a_0 0·11023 e_0 -0·01821 $dC_L/d\alpha$ = 2·396
c_0 -0·01006 p_0 -0·00350 Local a.c. 0·25 chord

η	K/4sV per rad	C_{LL}	η	K/4sV per rad	C_{LL}
0	0·344	0·664	0·6	0·262	1·260
0·1	0·343	0·734	0·7	0·226	1·452
0·2	0·337	0·812	0·8	0·181	1·747
0·3	0·326	0·898	0·9	0·123	2·375
0·4	0·311	0·998	0·95	0·084	3·258
0·5	0·289	1·115	1·0	0	

Table 29
Solution 10 126 vortex incidence
8 point unconditional

a_0 0·10641 e_0 -0·08009
a_1 0·01679 e_1 0·13761
c_0 0·05632 p_0 -0·22086
c_1 -0·14087 p_1 0·45148
$dc_L/d\alpha$ = 2·503 a.c. 1·180 $\bar{c}$ behind apex

η	K/4sV per rad.	C_{LL}	Local a.c.	η	K/4sV per rad.	C_{LL}	Local a.c.
0	0·362	0·668	0·364	0·55	0·287	1·176	0·266
0·05	0·361	0·702	0·346	0·60	0·272	1·253	0·261
0·10	0·359	0·736	0·333	0·65	0·255	1·342	0·258
0·15	0·356	0·773	0·322	0·70	0·236	1·448	0·255
0·20	0·352	0·811	0·312	0·75	0·214	1·581	0·254
0·25	0·346	0·852	0·304	0·80	0·190	1·756	0·256
0·30	0·340	0·896	0·297	0·85	0·163	2·005	0·259
0·35	0·332	0·942	0·290	0·90	0·131	2·419	0·267
0·40	0·323	0·993	0·284	0·95	0·091	3·363	0·278
0·45	0·312	1·048	0·277	1·00	0		0·295
0·50	0·300	1·109	0·271				

Table 30
Solution 11 126 vortex incidence
8 point unconditional, simplified lattice

a_0 0·11263 e_0 -0·09512
a_1 0·01826 e_1 0·17459
c_0 0·06476 p_0 -0·26246
c_1 -0·17007 p_1 0·54181
$dc_L/d\alpha$ = 2·596 a.c. 1·181 $\bar{c}$ behind apex

η	K/4sV per rad.	C_{LL}	Local a.c.	η	K/4sV per rad.	C_{LL}	Local a.c.
0	0·379	0·674	0·364	0·55	0·296	1·171	0·263
0·05	0·378	0·708	0·355	0·60	0·280	1·246	0·258
0·10	0·376	0·742	0·340	0·66	0·262	1·352	0·254
0·15	0·372	0·778	0·327	0·70	0·242	1·456	0·252
0·20	0·367	0·816	0·316	0·75	0·220	1·565	0·251
0·25	0·361	0·856	0·307	0·80	0·195	1·737	0·254
0·30	0·354	0·899	0·298	0·85	0·167	1·984	0·260
0·35	0·345	0·944	0·290	0·90	0·134	2·394	0·270
0·40	0·335	0·994	0·283	0·95	0·093	3·322	0·285
0·45	0·324	1·047	0·276	1·00	0		0·307
0·50	0·311	1·106	0·269				

Table 31 Solution 12 126 vortex incidence

10 point unconditional

a_0 0·10677 e_0 −0·07161 $dc_L/d\alpha = 2·503$
a_1 0·01481 e_1 0·11852
c_0 0·05001 p_0 −0·22200
c_1 −0·12638 p_1 0·45542
a.c. 1·181 $\bar{c}$ behind apex

η	K/4sV per rad	c_{LL}	Local a.c.	η	K/4sV per rad	c_{LL}	Local a.c.
0	0·362	0·668	0·354	0·55	0·287	1·177	0·268
0·05	0·361	0·701	0·346	0·60	0·272	1·254	0·264
0·10	0·359	0·736	0·333	0·65	0·255	1·343	0·260
0·15	0·356	0·772	0·322	0·70	0·236	1·450	0·257
0·20	0·352	0·811	0·312	0·75	0·214	1·582	0·256
0·25	0·346	0·852	0·305	0·80	0·190	1·756	0·256
0·30	0·340	0·896	0·298	0·85	0·163	2·005	0·259
0·35	0·332	0·942	0·291	0·90	0·131	2·417	0·265
0·40	0·323	0·993	0·285	0·95	0·091	3·347	0·274
0·45	0·312	1·048	0·279	1·00	0		0·287
0·50	0·301	1·109	0·273				

Table 32 Solution 13 126 vortex incidence

8 point conditional $p_0 + \frac{1}{2}p_1 = 0$

a_0 0·10372 e_0 −0·08947 $dc_L/d\alpha = 2·512$
a_1 0·02376 e_1 0·16269 $c_{Di} = 0·1390\, c_L^2$
c_0 0·06581 p_0 −0·21005
c_1 −0·16669 p_1 0·42010
a.c. 1·183 $\bar{c}$ behind apex

η	K/4sV per rad	c_{LL}	Local a.c.	η	K/4sV per rad	c_{LL}	Local a.c.
0	0·363	0·668	0·356	0·55	0·288	1·175	0·266
0·05	0·363	0·702	0·349	0·60	0·272	1·251	0·261
0·10	0·361	0·737	0·336	0·65	0·255	1·339	0·257
0·15	0·358	0·774	0·326	0·70	0·236	1·445	0·255
0·20	0·354	0·813	0·316	0·75	0·214	1·577	0·254
0·25	0·348	0·854	0·308	0·80	0·190	1·752	0·256
0·30	0·342	0·897	0·300	0·85	0·163	2·003	0·261
0·35	0·334	0·944	0·293	0·90	0·132	2·419	0·269
0·40	0·324	0·994	0·286	0·95	0·091	3·361	0·283
0·45	0·313	1·048	0·279	1·00	0		0·303
0·50	0·301	1·108	0·272				

Table 33 Solution 14 126 vertex incidence

8 point conditional:- $a_1 + c_1 + e_1 + 0.04306\, p_1 = 0$ and $p_0 + \tfrac{1}{2} p_1 = 0$

a_0	0·10493	e_0	−0·05158	$dC_L/d\alpha = 2.517$
a_1	0·02111	e_1	0·06931	
c_0	0·04263	p_0	−0·21402	
c_1	−0·10884	p_1	0·42804	

a.c. 1·185 $\bar{c}$ behind apex

η	K/4sV per rad.	C_{LL}	Local a.c.	η	K/4sV per rad.	C_{LL}	Local a.c.
0	0·363	0·666	0·355	0·55	0·290	1·181	0·274
0·05	0·362	0·700	0·348	0·60	0·274	1·257	0·269
0·10	0·361	0·735	0·336	0·65	0·257	1·345	0·264
0·15	0·358	0·773	0·325	0·70	0·237	1·450	0·259
0·20	0·354	0·812	0·316	0·75	0·215	1·579	0·255
0·25	0·349	0·854	0·309	0·80	0·190	1·747	0·251
0·30	0·342	0·898	0·303	0·85	0·162	1·987	0·249
0·35	0·335	0·945	0·297	0·90	0·130	2·383	0·248
0·40	0·326	0·997	0·291	0·95	0·089	3·278	0·248
0·45	0·315	1·052	0·285	1·00	0		0·250
0·50	0·303	1·113	0·280				

Table 34 Solution 15, lifting line solution for incidence

A_1	0·4360	$dC_L/d\alpha \equiv 3.163$	
A_3	−0·0625	$C_{Di} = 0.1468\, C_L^2$	
A_5	−0·0076	Local a.c. 0·25 chord.	
A_7	−0·0069	a.c. 1·083 $\bar{c}$ behind apex	

η	K/4sV per rad.	C_{LL}	η	K/4sV per rad.	C_{LL}
0	0·498	0·727	0·55	0·356	1·157
0·05	0·496	0·763	0·60	0·333	1·215
0·10	0·492	0·798	0·65	0·307	1·281
0·15	0·485	0·834	0·70	0·279	1·356
0·20	0·476	0·868	0·75	0·247	1·440
0·25	0·464	0·903	0·80	0·210	1·536
0·30	0·450	0·939	0·85	0·169	1·649
0·35	0·434	0·976	0·90	0·123	1·800
0·40	0·417	1·015	0·95	0·072	2·107
0·45	0·398	1·058	1·00	0	
0·50	0·378	1·104			

Table 35 Solution 16 21 vortex linear wing twist

a_o − 0·01295 α_o −0·3973

c_o 0·07107 C_{mo} −0·0970

e_o − 0·03851 Local a.c. 0·25 chord.

η	K/4sV per rad	K/4sV for C_{mo}=-0·1	η	K/4sV per rad	K/4sV for C_{mo}=-0·1
0	−0·0407	−0·0420	0·55	0·0132	0·0136
0·05	−0·0401	−0·0413	0·60	0·0192	0·0198
0·10	−0·0383	−0·0395	0·65	0·0243	0·0251
0·15	−0·0353	−0·0365	0·70	0·0283	0·0292
0·20	−0·0313	−0·0323	0·75	0·0309	0·0318
0·25	−0·0263	−0·0272	0·80	0·0316	0·0326
0·30	−0·0205	−0·0212	0·85	0·0303	0·0312
0·35	−0·0142	−0·0146	0·90	0·0265	0·0273
0·40	−0·0074	−0·0076	0·95	0·0194	0·0201
0·45	−0·0004	−0·0004	1·00	0	0
0·50	0·0066	0·0068			

Table 36 Solution 17 126 vortex linear wing twist

a_o −0·02148 e_o −0·03909

a_1 0·01683 e_1 0·01363

c_o 0·08331 α_o −0·3932

c_1 −0·02978 C_{mo} −0·1442

η	K/4sV per rad	K/4sV for C_{mo}=-0·1	Local a.c.	η	K/4sV per rad	K/4sV for C_{mo}=-0·1	Local a.c.
0	−0·0411	−0·0285	0·089	0·55	0·0123	0·0085	0·492
0·05	−0·0405	−0·0281	0·088	0·60	0·0185	0·0129	0·384
0·10	−0·0387	−0·0269	0·083	0·65	0·0241	0·0167	0·333
0·15	−0·0359	−0·0249	0·075	0·70	0·0285	0·0198	0·304
0·20	−0·0320	−0·0222	0·062	0·75	0·0316	0·0219	0·286
0·25	−0·0271	−0·0188	0·040	0·80	0·0330	0·0229	0·274
0·30	−0·0215	−0·0149	0·002	0·85	0·0323	0·0224	0·266
0·35	−0·0152	−0·0105	−0·073	0·90	0·0290	0·0201	0·260
0·40	−0·0085	−0·0059	−0·275	0·95	0·0220	0·0152	0·256
0·45	−0·0015	−0·0010	−2·391	1·00	0	0	0·254
0·50	0·0055	0·0038	0·883				

Table 37 Solution 18 328 vortex linear wing twist

a_0 −0·02201 C_0 0·08395 e_0 −0·04057 α_0 −0·3944
a_1 0·01740 C_1 −0·01994 e_1 −0·00182 C_{m_0} −0·1464
a_2 0·00060 C_2 −0·01141 e_2 0·02032

η	K/4sV per rad.	K/4sV For C_{m_0}=-01	Local a.c	η	K/4sV per rad.	K/4sV For C_{m_0}=-0·1	Local a.c.
0	−0·0418	−0·0286	0·092	0·55	0·0138	0·0094	0·540
0·05	−0·0412	−0·0281	0·090	0·60	0·0200	0·0136	0·421
0·10	−0·0393	−0·0269	0·084	0·65	0·0252	0·0172	0·360
0·15	−0·0363	−0·0248	0·072	0·70	0·0291	0·0199	0·320
0·20	−0·0321	−0·0219	0·053	0·75	0·0315	0·0215	0·291
0·25	−0·0269	−0·0184	0·022	0·80	0·0321	0·0220	0·267
0·30	−0·0209	−0·0143	−0·034	0·85	0·0306	0·0209	0·244
0·35	−0·0143	−0·0098	−0·146	0·90	0·0266	0·0182	0·220
0·40	−0·0073	−0·0050	−0·482	0·95	0·0193	0·0132	0·193
0·45	−0·0001	−0·0001	−Large	1·00	0	0	0·160
0·50	0·0071	0·0048	0·889				

Table 38 Solution 19 126 vortex linear wing twist

a_0' 0·00238 p_{b_0} −0·02343 C_{m_0} −0·1591
a_1' 0·00028 p_{b_1} 0·01339
p_{a_0} −0·00454 Increment of α_0 0·04333
p_{a_1} −0·00207 Total α_0 −0·3498

η	K/4sV per rad.	K/4sV For C_{m_0}=-01	Local a.c.	η	K/4sV per rad	K/4sV For C_{m_0}=-01	Local a.c.
0	−0·0485	−0·0305	0·088	0·55	0·0140	0·0088	0·494
0·05	−0·0470	−0·0295	0·085	0·60	0·0205	0·0129	0·334
0·10	−0·0436	−0·0274	0·077	0·65	0·0261	0·0164	0·333
0·15	−0·0391	−0·0246	0·065	0·70	0·0305	0·0192	0·304
0·20	−0·0337	−0·0212	0·047	0·75	0·0336	0·0211	0·286
0·25	−0·0279	−0·0175	0·019	0·80	0·0349	0·0219	0·274
0·30	−0·0215	−0·0135	−0·029	0·85	0·0341	0·0214	0·266
0·35	−0·0147	−0·0092	−0·127	0·90	0·0306	0·0192	0·260
0·40	−0·0076	−0·0048	−0·415	0·95	0·0231	0·0145	0·256
0·45	−0·0002	−0·0001	−Large	1·00	0	0	0·254
0·50	0·0071	0·0045	0·809				

Table 39 Solution 20 126 Vortex linear wing twist

a_0' 0·00213 Increment of α_0 0·03743

a_1' 0·00086 Total α_0 − 0·3558

p_0 −0·02641 C_{mo} − 0·1540

p_1 0·00798

η	K/4sV per rad	K/4sV for C_{mo}=-0·1	Local a.c.	η	K/4sV per rad	K/4sV for C_{mo}=-0·1	Local a.c.
0	-0·0487	-0·0316	0·089	0·55	0·0141	0·0092	0·492
0·05	-0·0472	-0·0306	0·088	0·60	0·0205	0·0133	0·384
0·10	-0·0438	-0·0284	0·083	0·65	0·0261	0·0169	0·333
0·15	-0·0392	-0·0255	0·075	0·70	0·0306	0·0199	0·304
0·20	-0·0338	-0·0219	0·062	0·75	0·0337	0·0219	0·286
0·25	-0·0279	-0·0181	0·040	0·80	0·0350	0·0227	0·274
0·30	-0·0215	-0·0140	0·002	0·85	0·0341	0·0221	0·266
0·35	-0·0147	-0·0095	-0·073	0·90	0·0306	0·0199	0·260
0·40	-0·0075	-0·0049	-0·276	0·95	0·0232	0·0151	0·256
0·45	-0·0002	-0·0001	-0·391	1·00	0	0	0·254
0·50	0·0071	0·0046	0·883				

Table 40 Solution 21 126 Vortex linear wing twist

a_0 − 0·01891 α_0 −0·03880 α_0 −0·3757

a_1 0·01699 a_1 0·01289 c_{mo} −0·1517

c_0 0·08273 p_0 −0·02123

c_1 −0·02919 p_1 −0·00258

η	K/4sV per rad	K/4sV for C_{mo}=-0·1	Local a.c.	η	K/4sV per rad	K/4sV for C_{mo}=-0·1	Local a.c.
0	-0·0484	-0·0318	0·117	0·55	0·0140	0·0092	0·464
0·05	-0·0470	-0·0310	0·113	0·60	0·0204	0·0134	0·373
0·10	-0·0436	-0·0287	0·104	0·65	0·0260	0·0171	0·328
0·15	-0·0390	-0·0257	0·091	0·70	0·0304	0·0200	0·302
0·20	-0·0336	-0·0221	0·072	0·75	0·0335	0·0221	0·286
0·25	-0·0277	-0·0183	0·046	0·80	0·0347	0·0229	0·273
0·30	-0·0214	-0·0141	0·002	0·85	0·0339	0·0223	0·265
0·35	-0·0146	-0·0096	-0·087	0·90	0·0303	0·0200	0·260
0·40	-0·0074	-0·0049	-0·350	0·95	0·0229	0·0151	0·256
0·45	-0·0001	-0·0001	- Large	1·00	0	0	0·253
0·50	0·0071	0·0047	0·743				

Table 41 Solution 22 Lifting line, twist solution

A_3 0·0799 α_0 −0·4235

A_5 0·0025 C_{mo} −0·2235

A_7 0·0180 Local a.c. 0·25 chord

η	K/4sV per rad	η	K/4sV per rad
0	−0·0954	0·55	0·0223
0·05	−0·0935	0·60	0·0293
0·10	−0·0880	0·65	0·0353
0·15	−0·0790	0·70	0·0410
0·20	−0·0673	0·75	0·0480
0·25	−0·0538	0·80	0·0570
0·30	−0·0390	0·85	0·0683
0·35	−0·0243	0·90	0·0796
0·40	−0·0102	0·95	0·0819
0·45	0·0026	1·00	0
0·50	0·0134		

Table 42

Summary of incidence solutions

Soln.	Description.	$dC_L/d\alpha$	a.c.	C_{Di}
1	21 vortex, 3 pt	2·402	1·116	$0·1392\ C_L^2$
2	21 vortex, 5 pt	2·408		$0·1392\ C_L^2$
3	126 vortex, 6 pt standard	2·618	1·160	$0·1390\ C_L^2$
4	126 vortex, 9 pt standard	2·499	1·168	$0·1388\ C_L^2$
5	328 vortex, 9 pt standard	2·606	1·162	$0·1392\ C_L^2$
6	328 vortex, 12 pt standard	2·614	1·163	$0·1392\ C_L^2$
7	126 vortex, 6 pt addition	2·518		$0·1390\ C_L^2$
8	126 vortex, 4 pt addition	2·518	1·183	$0·1390\ C_L^2$
9	21 vortex, 4 pt	2·396		
10	126 vortex, 8 pt	2·503	1·180	
11	126 vortex, 8 pt	2·596	1·181	
12	126 vortex, 10 pt	2·503	1·181	
13	126 vortex, 8 pt	2·512	1·183	$0·1390\ C_L^2$
14	126 vortex, 8 pt	2·517	1·185	
15	Lifting line	3·163	1·083	$0·1468\ C_L^2$

Table 43

Summary of wing twist solutions

Soln.	Description	α_o	C_{mo}
16	21 vortex, 3 pt	−0·397	−0·097
17	126 vortex, 6 pt standard	−0·393	−0·144
18	328 vortex, 12 pt standard solution	−0·394	−0·146
19	126 vortex, 6 pt addition	−0·350	−0·159
21	126 vortex, 6 pt addition	−0·356	−0·154
22	126 vortex, 8 pt solution	−0·376	−0·152
23	Lifting line	−0·424	−0·224

Table 44.

Downwash factors for lifting line lattice.

VORTEX / POINT	K_{10}	K_9	K_8	K_7	K_6	K_5	K_4	K_3	K_2	K_1	K_0	K_1	K_2	K_3	K_4	K_5	K_6	K_7	K_8	K_9	K_{10}
0	$\bar{0}$·0013	$\bar{0}$·0062	$\bar{0}$·0078	$\bar{0}$·0103	$\bar{0}$·0140	$\bar{0}$·0202	$\bar{0}$·0317	$\bar{0}$·0571	$\bar{0}$·1333	$\bar{0}$·6667	2·0000	$\bar{0}$·6667	$\bar{0}$·1333	$\bar{0}$·0571	$\bar{0}$·0317	$\bar{0}$·0202	$\bar{0}$·0140	$\bar{0}$·0103	$\bar{0}$·0078	$\bar{0}$·0062	$\bar{0}$·0013
1	$\bar{0}$·0011	$\bar{0}$·0050	$\bar{0}$·0062	$\bar{0}$·0078	$\bar{0}$·0103	$\bar{0}$·0140	$\bar{0}$·0202	$\bar{0}$·0317	$\bar{0}$·0571	$\bar{0}$·1333	$\bar{0}$·6667	2·0000	$\bar{0}$·6667	$\bar{0}$·1333	$\bar{0}$·0571	$\bar{0}$·0317	$\bar{0}$·0202	$\bar{0}$·0140	$\bar{0}$·0103	$\bar{0}$·0078	$\bar{0}$·0017
2	$\bar{0}$·0009	$\bar{0}$·0041	$\bar{0}$·0050	$\bar{0}$·0062	$\bar{0}$·0078	$\bar{0}$·0103	$\bar{0}$·0140	$\bar{0}$·0202	$\bar{0}$·0317	$\bar{0}$·0571	$\bar{0}$·1333	$\bar{0}$·6667	2·0000	$\bar{0}$·6667	$\bar{0}$·1333	$\bar{0}$·0571	$\bar{0}$·0317	$\bar{0}$·0202	$\bar{0}$·0140	$\bar{0}$·0103	$\bar{0}$·0022
3	$\bar{0}$·0008	$\bar{0}$·0035	$\bar{0}$·0041	$\bar{0}$·0050	$\bar{0}$·0062	$\bar{0}$·0078	$\bar{0}$·0103	$\bar{0}$·0140	$\bar{0}$·0202	$\bar{0}$·0317	$\bar{0}$·0571	$\bar{0}$·1333	$\bar{0}$·6667	2·0000	$\bar{0}$·6667	$\bar{0}$·1333	$\bar{0}$·0571	$\bar{0}$·0317	$\bar{0}$·0202	$\bar{0}$·0140	$\bar{0}$·0028
4	$\bar{0}$·0007	$\bar{0}$·0030	$\bar{0}$·0035	$\bar{0}$·0041	$\bar{0}$·0050	$\bar{0}$·0062	$\bar{0}$·0078	$\bar{0}$·0103	$\bar{0}$·0140	$\bar{0}$·0202	$\bar{0}$·0317	$\bar{0}$·0571	$\bar{0}$·1333	$\bar{0}$·6667	2·0000	$\bar{0}$·6667	$\bar{0}$·1333	$\bar{0}$·0571	$\bar{0}$·0317	$\bar{0}$·0202	$\bar{0}$·0040
5	$\bar{0}$·0006	$\bar{0}$·0026	$\bar{0}$·0030	$\bar{0}$·0035	$\bar{0}$·0041	$\bar{0}$·0050	$\bar{0}$·0062	$\bar{0}$·0078	$\bar{0}$·0103	$\bar{0}$·0140	$\bar{0}$·0202	$\bar{0}$·0317	$\bar{0}$·0571	$\bar{0}$·1333	$\bar{0}$·6667	2·0000	$\bar{0}$·6667	$\bar{0}$·1333	$\bar{0}$·0571	$\bar{0}$·0317	$\bar{0}$·0058
6	$\bar{0}$·0005	$\bar{0}$·0022	$\bar{0}$·0026	$\bar{0}$·0030	$\bar{0}$·0035	$\bar{0}$·0041	$\bar{0}$·0050	$\bar{0}$·0062	$\bar{0}$·0078	$\bar{0}$·0103	$\bar{0}$·0140	$\bar{0}$·0202	$\bar{0}$·0317	$\bar{0}$·0571	$\bar{0}$·1333	$\bar{0}$·6667	2·0000	$\bar{0}$·6667	$\bar{0}$·1333	$\bar{0}$·0571	$\bar{0}$·0095
7	$\bar{0}$·0005	$\bar{0}$·0020	$\bar{0}$·0022	$\bar{0}$·0026	$\bar{0}$·0030	$\bar{0}$·0035	$\bar{0}$·0041	$\bar{0}$·0050	$\bar{0}$·0062	$\bar{0}$·0078	$\bar{0}$·0103	$\bar{0}$·0140	$\bar{0}$·0202	$\bar{0}$·0317	$\bar{0}$·0571	$\bar{0}$·1333	$\bar{0}$·6667	2·0000	$\bar{0}$·6667	$\bar{0}$·1333	$\bar{0}$·0182
8	$\bar{0}$·0004	$\bar{0}$·0017	$\bar{0}$·0020	$\bar{0}$·0022	$\bar{0}$·0026	$\bar{0}$·0030	$\bar{0}$·0035	$\bar{0}$·0041	$\bar{0}$·0050	$\bar{0}$·0062	$\bar{0}$·0078	$\bar{0}$·0103	$\bar{0}$·0140	$\bar{0}$·0202	$\bar{0}$·0317	$\bar{0}$·0571	$\bar{0}$·1333	$\bar{0}$·6667	2·0000	$\bar{0}$·6667	$\bar{0}$·0476

Table 45 Equations for the determination of a lattice of vortices for a given distribution of downwash

Point	K_0	K_1	K_2	K_3	K_4	K_5	K_6	K_7	K_8	K_9	K_{10}	Const.Col. for Pa	Const.Col. for Pb	
0	2·0000	−1·3334	−0·2666	−0·1142	−0·0634	−0·0404	−0·0280	−0·0206	−0·0156	−0·0124	−0·0026	0·15708	0·15708	
1	−0·6667	1·8667	−0·7238	−0·1650	−0·0773	−0·0457	−0·0305	−0·0218	−0·0165	−0·0128	−0·0028	0	0·07854	
2	−0·1333	−0·7238	1·9683	−0·6869	−0·1473	−0·0674	−0·0395	−0·0264	−0·0190	−0·0144	−0·0031	0	0	
3	−0·0571	−0·1650	−0·6869	1·9860	−0·6770	−0·1411	−0·0633	−0·0367	−0·0243	−0·0175	−0·0036	0	0	
4	−0·0317	−0·0773	−0·1473	−0·6770	1·9922	−0·6729	−0·1383	−0·0612	−0·0352	−0·0232	−0·0047	0	0	= 0
5	−0·0202	−0·0457	−0·0674	−0·1411	−0·6729	1·9950	−0·6708	−0·1368	−0·0601	−0·0343	−0·0064	0	0	
6	−0·0140	−0·0305	−0·0395	−0·0633	−0·1383	−0·6708	1·9965	−0·6697	−0·1359	−0·0593	−0·0100	0	0	
7	−0·0103	−0·0218	−0·0264	−0·0367	−0·0612	−0·1368	−0·6697	1·9974	−0·6689	−0·1353	−0·0187	0	0	
8	−0·0078	−0·0165	−0·0190	−0·0243	−0·0352	−0·0601	−0·1359	−0·6689	1·9980	−0·6684	−0·0480	0	0	

A7428 Wt. 15 1,014 7/51 Gp. 959 Fosh & Cross Ltd., London.

Table 46

True and special values of P Functions used in the analysis

η	P_a		P_b	
	True	0·1 Lattice	True	0·1 Lattice
0	0·14308	0·1578	0·24197	0·2518
0·05	0·12579		0·23047	
0·10	0·09888	0·0940	0·20726	0·2092
0·15	0·08356		0·17952	
0·20	0·07366	0·0726	0·15307	0·1493
0·25	0·06610		0·13523	
0·30	0·05994	0·0594	0·12179	0·1206
0·35	0·05467		0·11067	
0·40	0·05003	0·0497	0·10104	0·1004
0·45	0·04584		0·09244	
0·50	0·04201	0·0418	0·08461	0·0841
0·55	0·03842		0·07731	
0·60	0·03504	0·0349	0·07043	0·0701
0·65	0·03176		0·06380	
0·70	0·02855	0·0284	0·05733	0·0571
0·75	0·02535		0·05089	
0·80	0·02209	0·0220	0·04433	0·0442
0·85	0·01866		0·03744	
0·90	0·01490	0·0149	0·02986	0·0299
0·95	0·01028		0·02064	
0·9625	0·00887	0·0089	0·01778	0·0178
1·00	0		0	

T_{15}	0·09992		0·19933	
T_{16}	0·50888		1·01517	
T_{19}	0·01595		0·03229	
T_{20}	0·03182		0·06386	

Table 46 cont.

η	$P = 0·65\ P_a + 0·35\ P_b$		$P = 0·2\ P_a + 0·8\ P_b$	
	True	0·1 lattice	True	0·1 lattice
0	0·17769	0·1907	0·22219	0·2330
0·05	0·16243		0·20953	
0·10	0·13681	0·1343	0·18558	0·1862
0·15	0·11715		0·16033	
0·20	0·10145	0·0994	0·13719	0·1340
0·25	0·09030		0·12140	
0·30	0·08159	0·0808	0·10942	0·1083
0·35	0·07427		0·09947	
0·40	0·06788	0·0674	0·09084	0·0902
0·45	0·06215		0·08312	
0·50	0·05692	0·0566	0·07609	0·0757
0·55	0·05203		0·06953	
0·60	0·04743	0·0472	0·06335	0·0631
0·65	0·04297		0·05739	
0·70	0·03862	0·0385	0·05157	0·0514
0·75	0·03429		0·04578	
0·80	0·02987	0·0298	0·03988	0·0398
0·85	0·02523		0·03368	
0·90	0·02014	0·0201	0·02687	0·0269
0·95	0·01391		0·01857	
0·9625	0·01199	0·0120	0·01600	0·0160
1·0000	0		0	

T_{15}	0·13471		0·17945	
T_{16}	0·68608		0·91391	
T_{19}	0·02167		0·02902	
T_{20}	0·04303		0·05745	

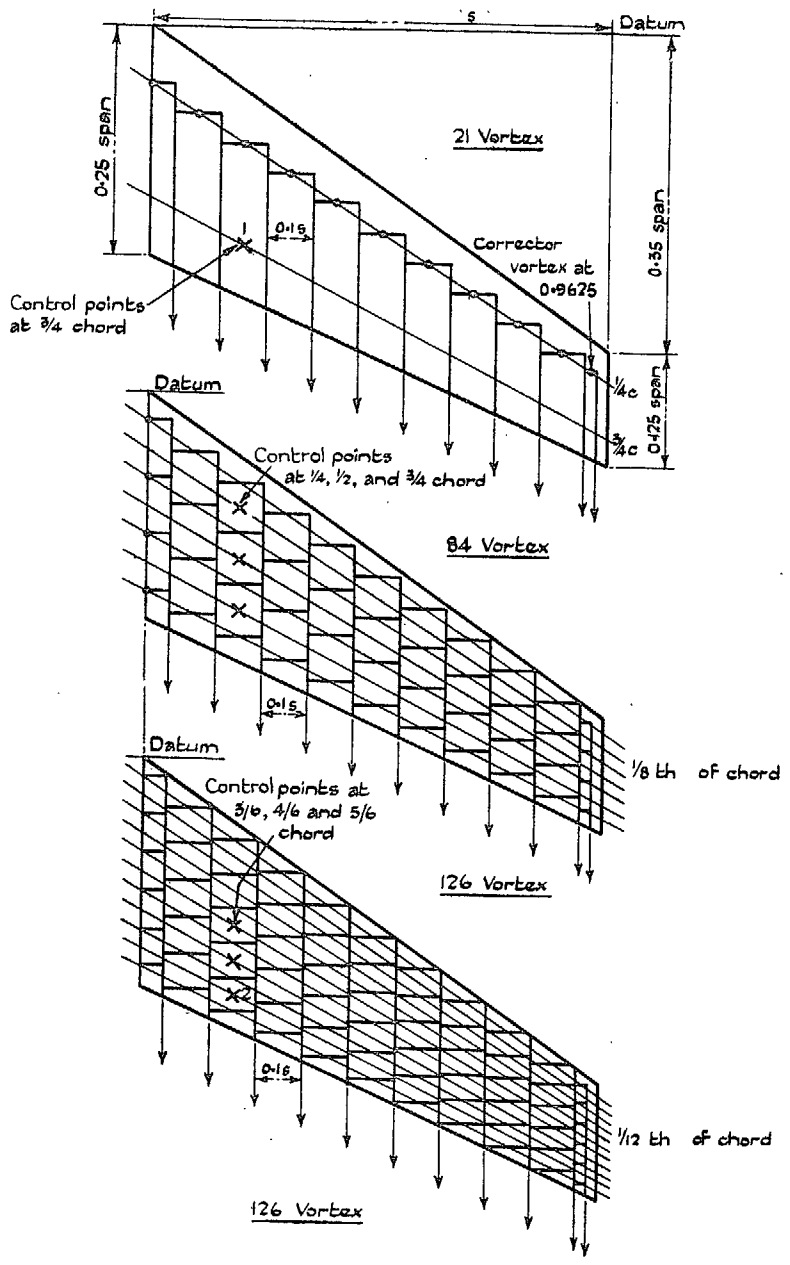

FIG. 1. Representation of half wing by vortex pattern.

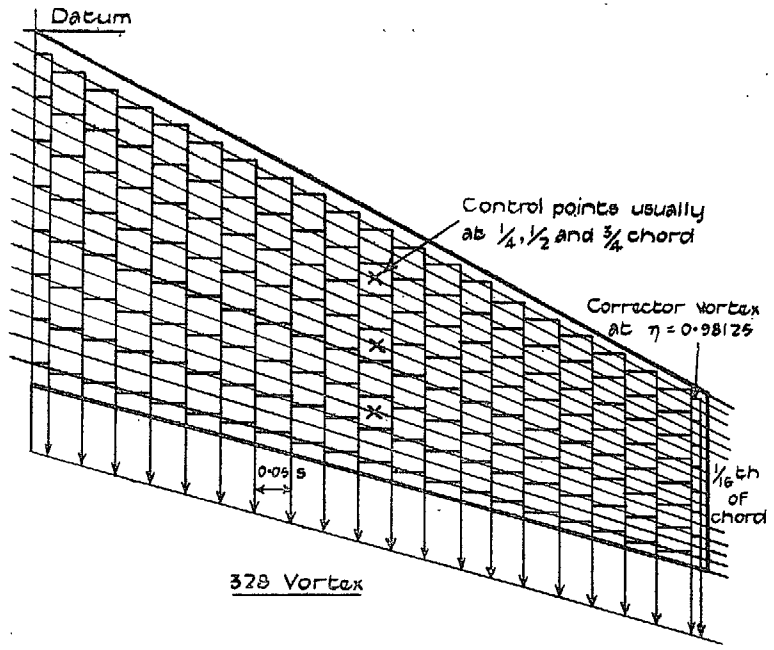

FIG. 2. Representation of half wing by vortex pattern.

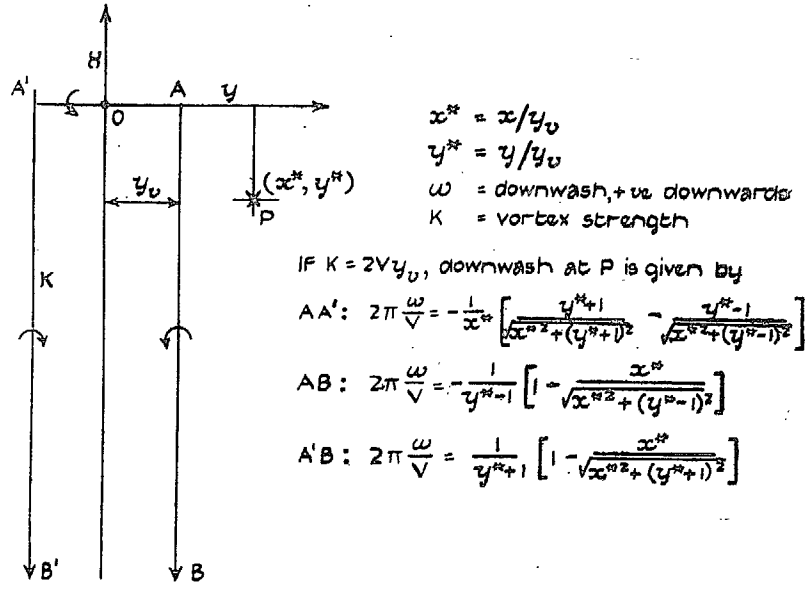

FIG. 3. Downwash due to a rectangular vortex.

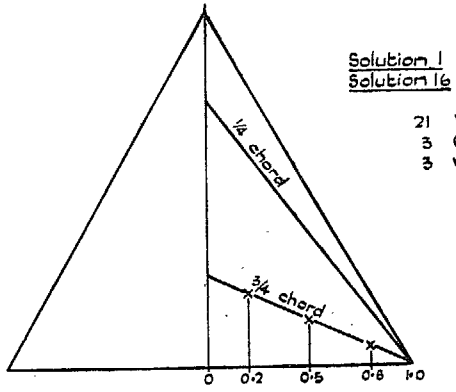

Solution 1 Incidence
Solution 16 Wing twist

21 Vortex
3 Control points
3 Variables :- a_0, c_0, e_0

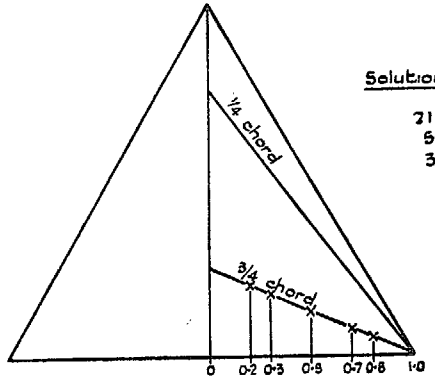

Solution 2 Incidence

21 Vortex
5 Control points
3 Variables - a_0, c_0, e_0

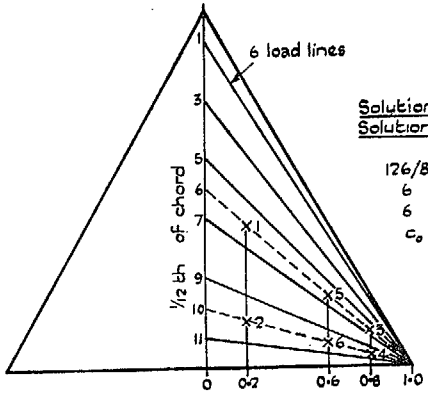

Solution 3 Incidence
Solution 17 Wing twist

126/86 vortex
6 Control points
6 variables :- $a_0, a_1,$
c_0, c_1, e_0, e_1

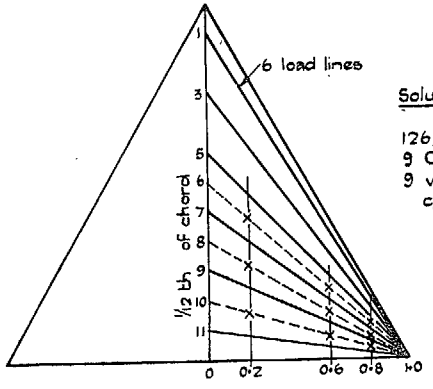

Solution 4 Incidence

126/86 vortex
9 Control points
9 variables :- a_0, a_1, a_2
$c_0, c_1, c_2, e_0, e_1, e_2$

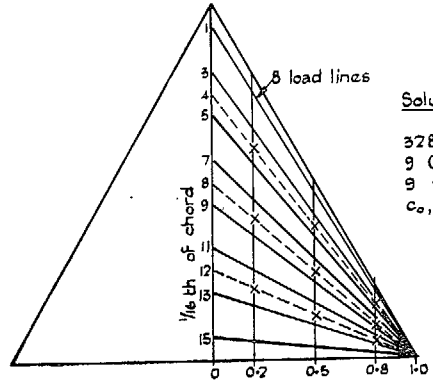

Solution 5 Incidence

328 vortex
9 Control points
9 variables :- a_0, a_1, a_2
$c_0, c_1, c_2, e_0, e_1, e_2$

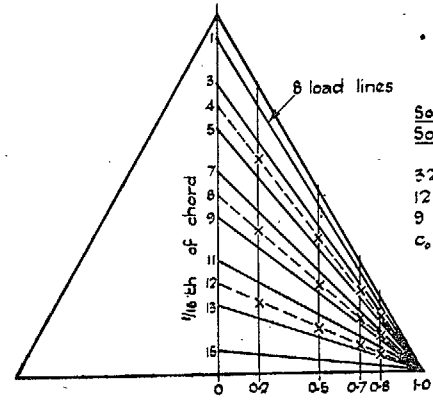

Solution 6 Incidence
Solution 18 Wing twist

328 vortex
12 Control points
9 variables :- $a_0, a_1, a_2,$
$c_0, c_1, c_2, e_0, e_1, e_2$

FIG. 4.

FIG. 5.

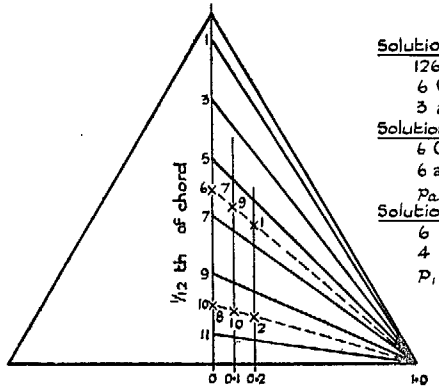

Solution 7 Incidence
126/86 vortex
6 Control points
3 additional variables: a_0', p_{a0}, p_{b0}

Solution 19 Wing twist
6 Control points
6 additional variables: a_1', p_{a0}, p_{a1}, p_{b0}, p_{b1}, a_0

Solution 20 Wing twist
6 Control points
4 additional variables: a_1', p_0, p_1, a_0

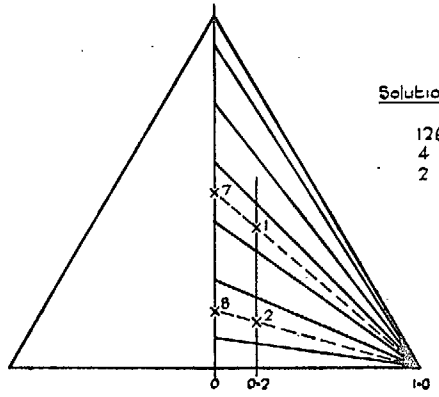

Solution 8 Incidence
126/86 vortex
4 Control points
2 additional variables: a_0', p_0

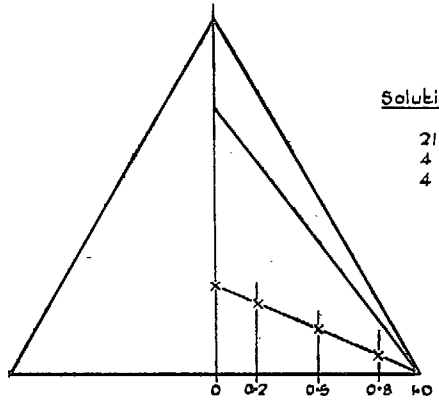

Solution 9 Incidence
21 vortex
4 Control points
4 variables: a_0, c_0, e_0, p_0

FIG. 6.

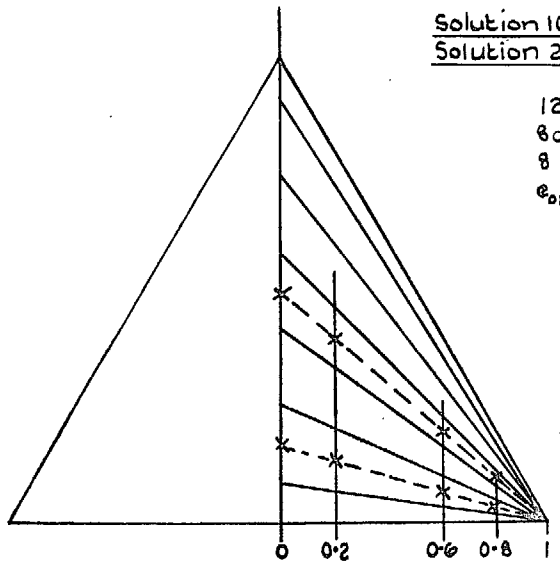

Solution 10, 11, 13, 14 Incidence
Solution 21 Wing twist

126/86 Vortex
8 control points
8 variables: $a_0, a_1, c_0, c_1, e_0, e_1, p_0, p_1$

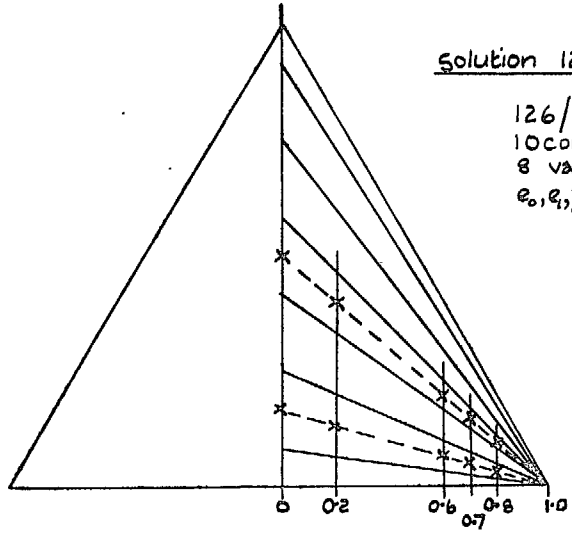

Solution 12 Incidence

126/86 Vortex
10 control points
8 variables: $a_0, a_1, c_0, c_1, e_0, e_1, p_0, p_1$

FIG. 7.

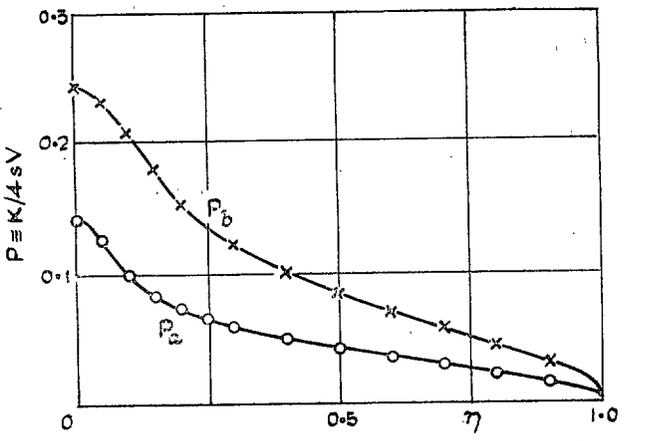

Symmetrical P Functions used in analysis

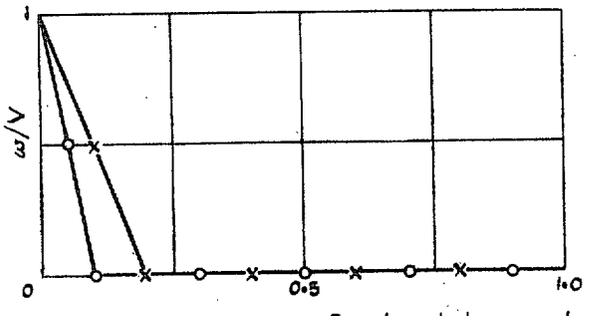

Corresponding curves of induced downwash

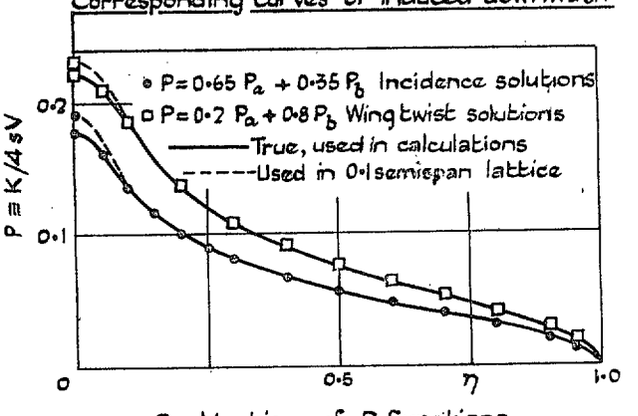

Combinations of P Functions

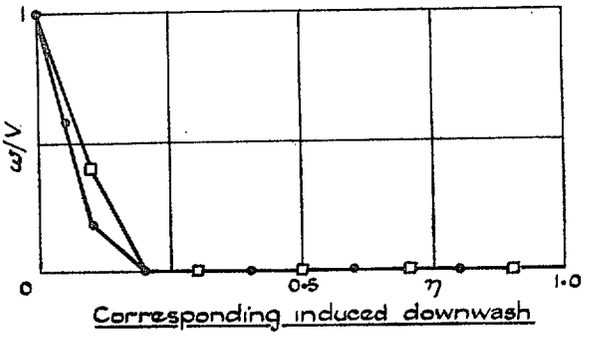

Corresponding induced downwash

FIG. 8.

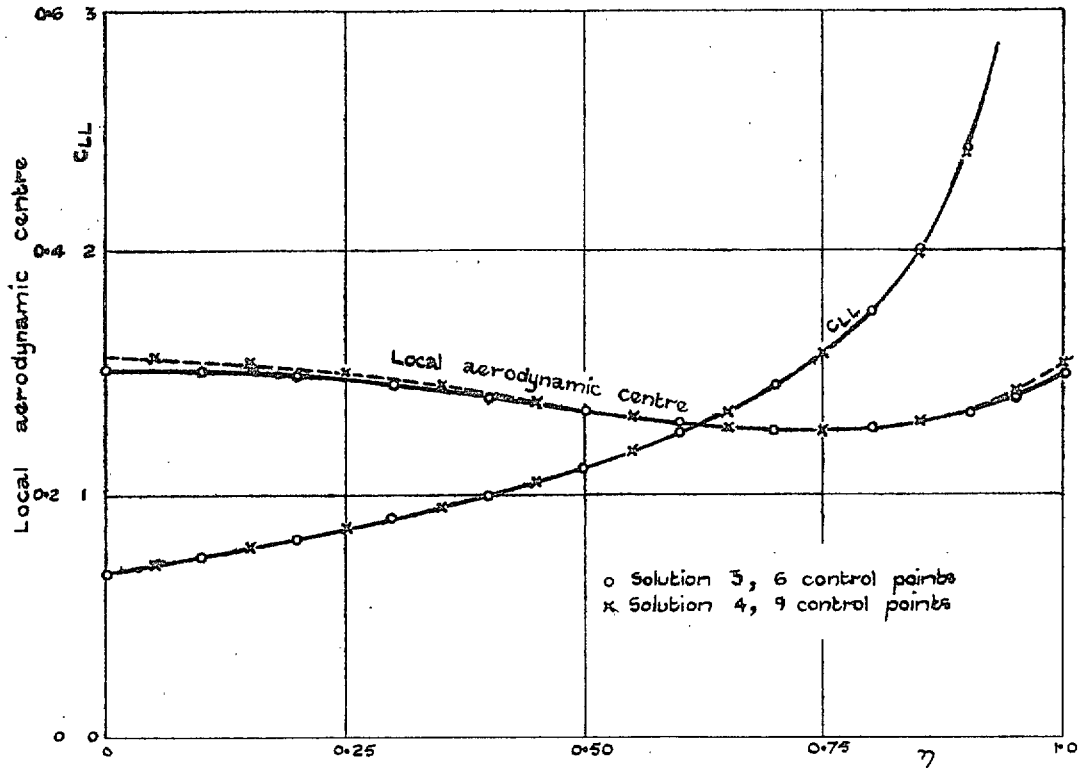

FIG. 9. Delta wing. Comparison of 126-vortex solutions for incidence.

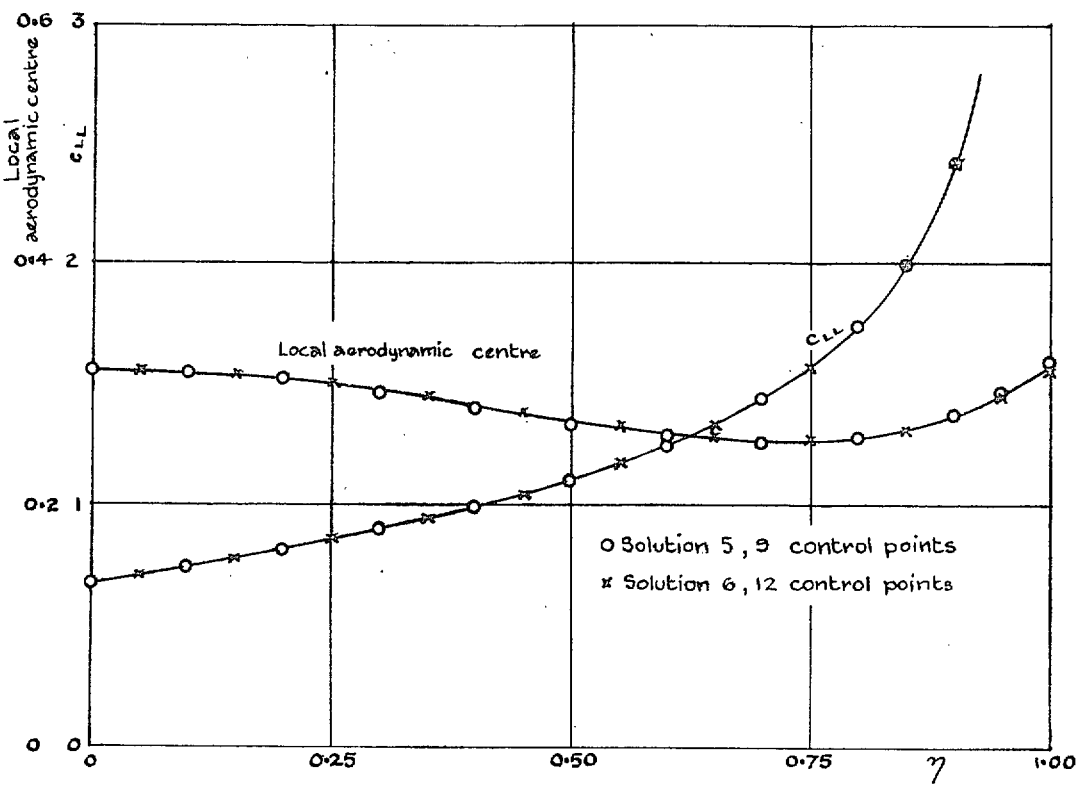

FIG. 10. Delta wing. Comparison of 328-vortex solutions for incidence.

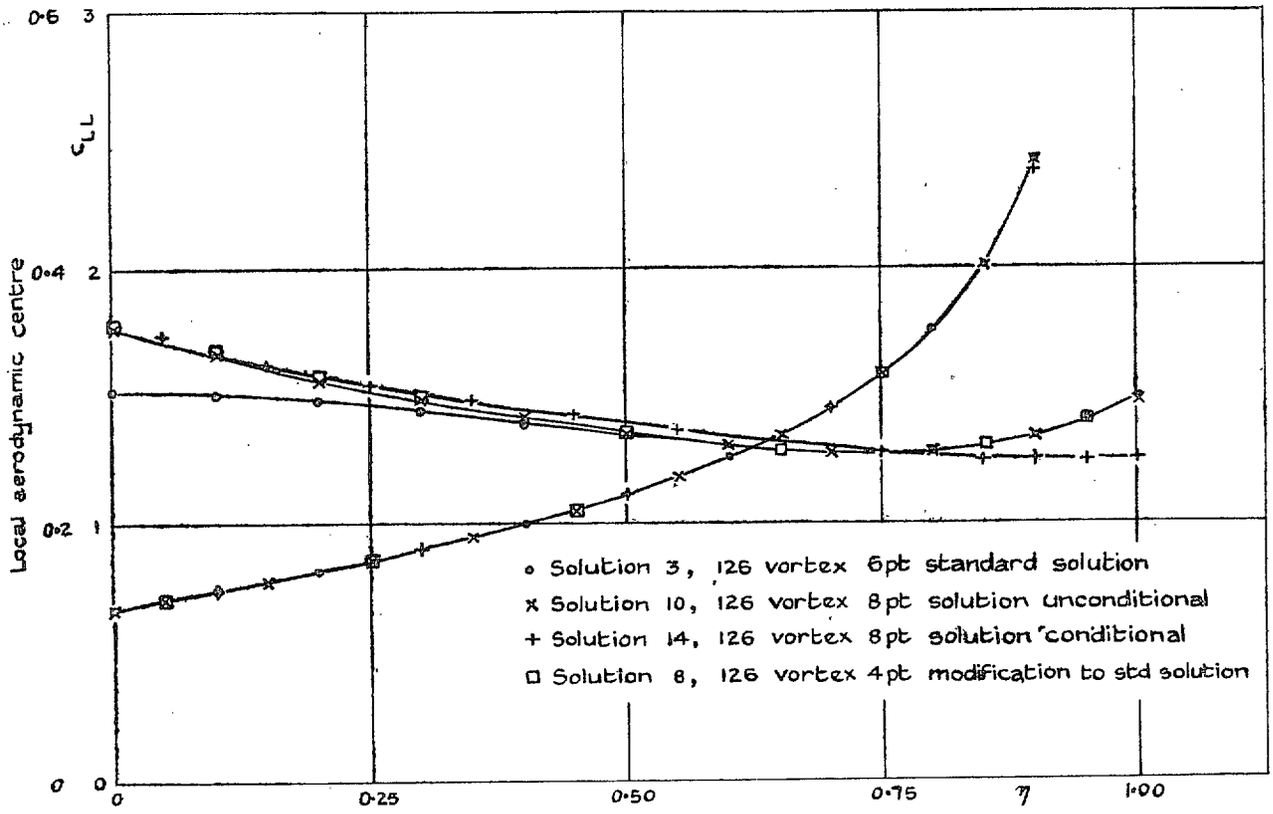

FIG. 11.

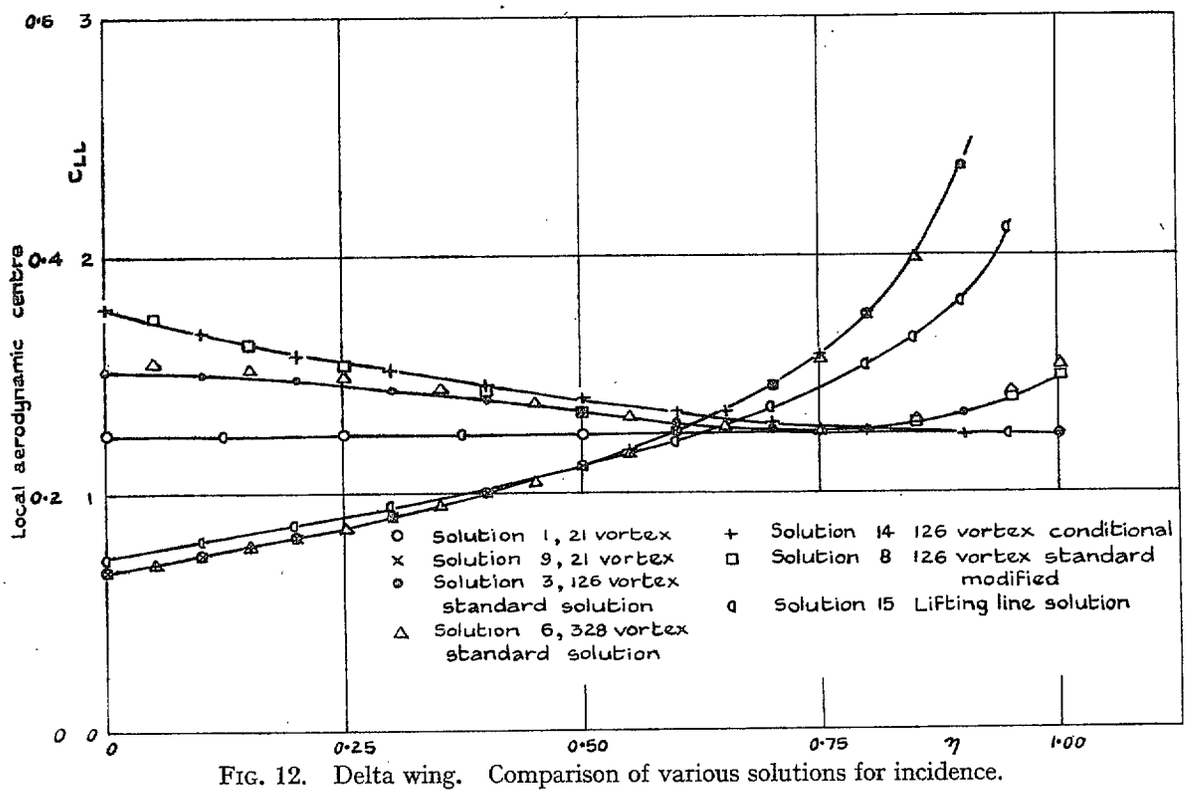

FIG. 12. Delta wing. Comparison of various solutions for incidence.

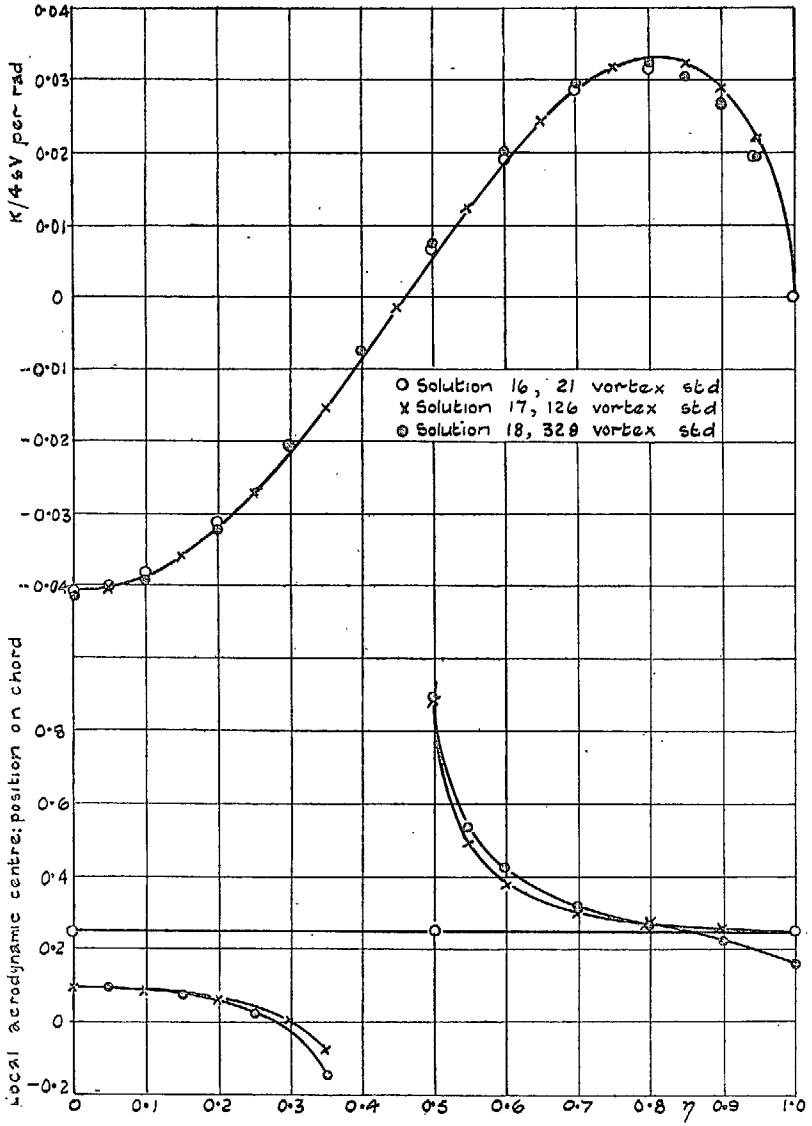

FIG. 13. Delta wing. Solutions for linear wing twist.

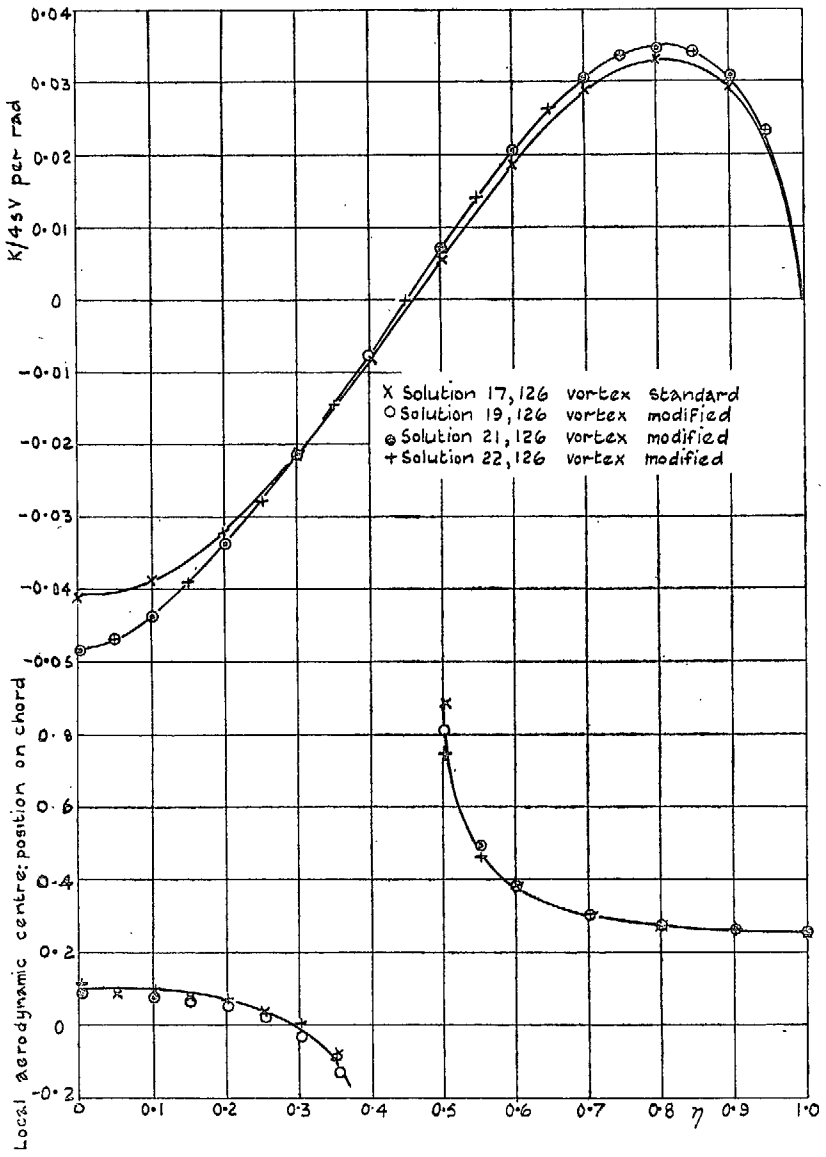

FIG. 14. Delta wing. Solutions for linear wing twist.

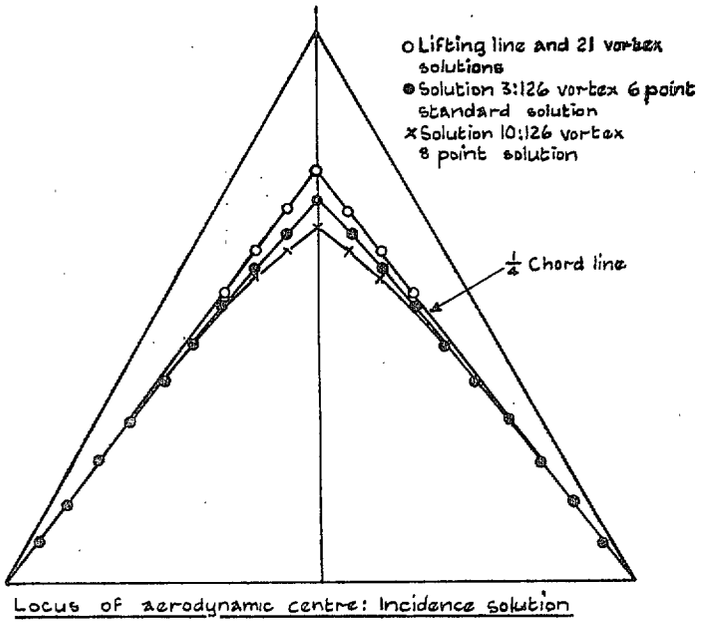

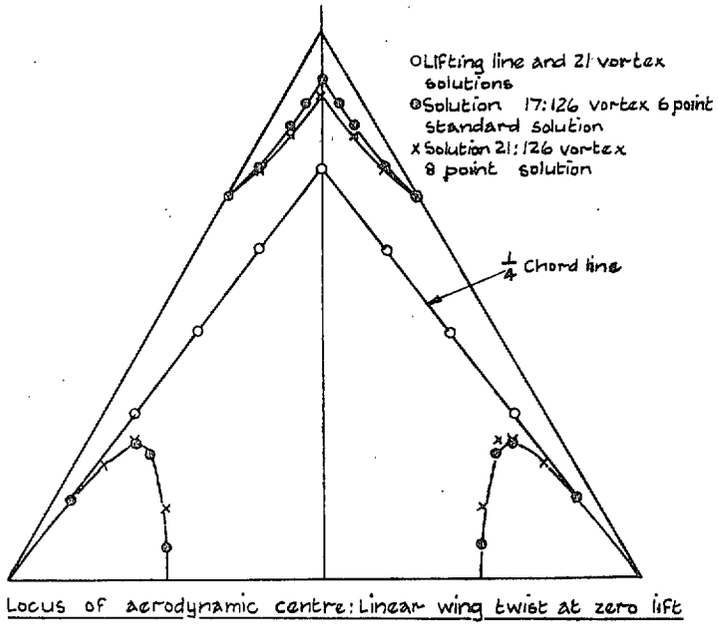

FIG. 15.

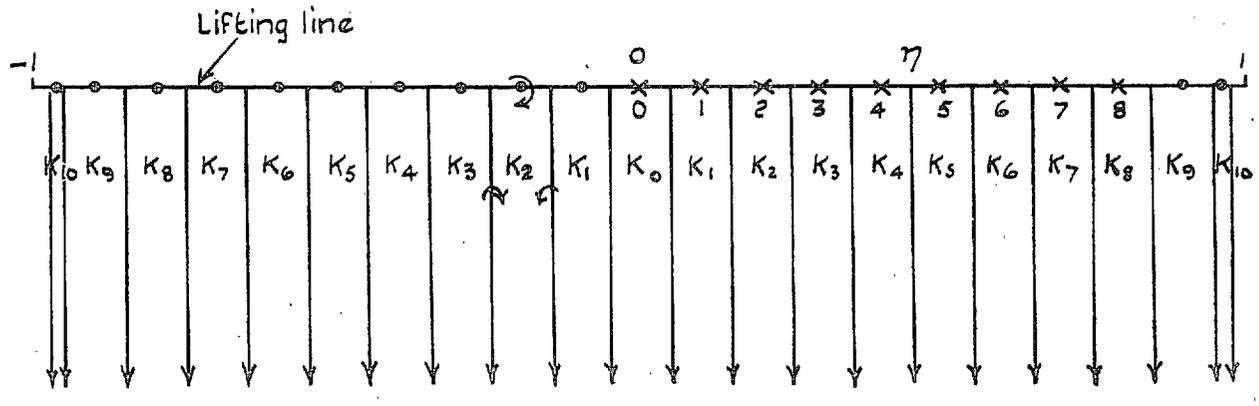

FIG. 16. Lattice to represent lifting line-theory.

(21060) Wt. 15-680 K9 12/52 F. M. & S. PRINTED IN GREAT BRITAIN

Publications of the Aeronautical Research Council

ANNUAL TECHNICAL REPORTS OF THE AERONAUTICAL RESEARCH COUNCIL (BOUND VOLUMES)—

1934–35 Vol. I. Aerodynamics. *Out of print.*
Vol. II. Seaplanes, Structures, Engines, Materials, etc. 40*s.* (40*s.* 8*d.*)

1935–36 Vol. I. Aerodynamics. 30*s.* (30*s.* 7*d.*)
Vol. II. Structures, Flutter, Engines, Seaplanes, etc. 30*s.* (30*s.* 7*d.*)

1936 Vol. I. Aerodynamics General, Performance, Airscrews, Flutter and Spinning. 40*s.* (40*s.* 9*d.*)
Vol. II. Stability and Control, Structures, Seaplanes, Engines, etc. 50*s.* (50*s.* 10*d.*)

1937 Vol. I. Aerodynamics General, Performance, Airscrews, Flutter and Spinning. 40*s.* (40*s.* 10*d.*)
Vol. II. Stability and Control, Structures, Seaplanes, Engines, etc. 60*s.* (61*s.*)

1938 Vol. I. Aerodynamics General, Performance, Airscrews. 50*s.* (51*s.*)
Vol. II. Stability and Control, Flutter, Structures, Seaplanes, Wind Tunnels, Materials. 30*s.* (30*s.* 9*d.*)

1939 Vol. I. Aerodynamics General, Performance, Airscrews, Engines. 50*s.* (50*s.* 11*d.*)
Vol. II. Stability and Control, Flutter and Vibration, Instruments, Structures, Seaplanes, etc. 63*s.* (64*s.* 2*d.*)

1940 Aero and Hydrodynamics, Aerofoils, Airscrews, Engines, Flutter, Icing, Stability and Control, Structures, and a miscellaneous section. 50*s.* (51*s.*)

Certain other reports proper to the 1940 *volume will subsequently be included in a separate volume.*

ANNUAL REPORTS OF THE AERONAUTICAL RESEARCH COUNCIL—

1933–34 1*s.* 6*d.* (1*s.* 8*d.*)
1934–35 1*s.* 6*d.* (1*s.* 8*d.*)
April 1, 1935 to December 31, 1936. 4*s.* (4*s.* 4*d.*)
1937 2*s.* (2*s.* 2*d.*)
1938 1*s.* 6*d.* (1*s.* 8*d.*)
1939–48 3*s.* (3*s.* 2*d.*)

INDEX TO ALL REPORTS AND MEMORANDA PUBLISHED IN THE ANNUAL TECHNICAL REPORTS, AND SEPARATELY—

April, 1950 R. & M. No. 2600. 2*s.* 6*d.* (2*s.* 7½*d.*)

INDEXES TO THE TECHNICAL REPORTS OF THE AERONAUTICAL RESEARCH COUNCIL—

December 1, 1936 — June 30, 1939. R. & M. No. 1850. 1*s.* 3*d.* (1*s.* 4½d.)
July 1, 1939 — June 30, 1945. R. & M. No. 1950. 1*s.* (1*s.* 1½*d.*)
July 1, 1945 — June 30, 1946. R. & M. No. 2050. 1*s.* (1*s.* 1½*d.*)
July 1, 1946 — December 31, 1946. R. & M. No. 2150. 1*s.* 3*d.* (1*s.* 4½*d.*)
January 1, 1947 — June 30, 1947. R. & M. No. 2250. 1*s.* 3*d.* (1*s.* 4½*d.*)

Prices in brackets include postage.

Obtainable from

HER MAJESTY'S STATIONERY OFFICE

York House, Kingsway, LONDON, W.C.2 423 Oxford Street, LONDON, W.1
P.O. Box 569, LONDON, S.E.1
13a Castle Street, EDINBURGH, 2 1 St. Andrew's Crescent, CARDIFF
39 King Street, MANCHESTER, 2 Tower Lane, BRISTOL, 1
2 Edmund Street, BIRMINGHAM, 3 80 Chichester Street, BELFAST

or through any bookseller.